



Tectonics

RESEARCH ARTICLE

10.1002/2015TC004052

Key Points:

- Multiple geochronometers were obtained for the Sarandí del Yí Shear Zone
- The Río de la Plata Craton and the Nico Pérez Terrane collided at 630–625 Ma
- Strain localization, magmatism, and fluids affect isotopic systems in mylonites

Supporting Information:

- Supporting Information S1
- Table S5

Correspondence to:

S. Oriolo,
seba.oriolo@gmail.com;
soriolo@gwdg.de

Citation:

Oriolo, S., P. Oyhantçabal, K. Wemmer, M. A. S. Basei, J. Benowitz, J. Pfänder, F. Hannich, and S. Siegesmund (2016), Timing of deformation in the Sarandí del Yí Shear Zone, Uruguay: Implications for the amalgamation of western Gondwana during the Neoproterozoic Brasiliano-Pan-African Orogeny, *Tectonics*, 35, 754–771, doi:10.1002/2015TC004052.

Received 8 OCT 2015

Accepted 4 MAR 2016

Accepted article online 11 MAR 2016

Published online 25 MAR 2016

Timing of deformation in the Sarandí del Yí Shear Zone, Uruguay: Implications for the amalgamation of western Gondwana during the Neoproterozoic Brasiliano-Pan-African Orogeny

Sebastián Oriolo¹, Pedro Oyhantçabal², Klaus Wemmer¹, Miguel A. S. Basei³, Jeffrey Benowitz⁴, Jörg Pfänder⁵, Felix Hannich¹, and Siegfried Siegesmund¹

¹Geoscience Center, Georg-August-Universität Göttingen, Göttingen, Germany, ²Departamento de Geología, Facultad de Ciencias, Universidad de la República, Montevideo, Uruguay, ³Instituto de Geociências, Universidade de São Paulo, São Paulo, Brazil, ⁴Geophysical Institute, University of Alaska Fairbanks, Fairbanks, Alaska, USA, ⁵Institut für Geologie, Technische Universität Bergakademie Freiberg, Freiberg, Germany

Abstract U-Pb and Hf zircon (sensitive high-resolution ion microprobe -SHRIMP- and laser ablation-inductively coupled plasma-mass spectrometry -LA-ICP-MS-), Ar/Ar hornblende and muscovite, and Rb-Sr whole rock-muscovite isochron data from the mylonites of the Sarandí del Yí Shear Zone, Uruguay, were obtained in order to assess the tectonothermal evolution of this crustal-scale structure. Integration of these results with available kinematic, structural, and microstructural data of the shear zone as well as with geochronological data from the adjacent blocks allowed to constrain the onset of deformation along the shear zone at 630–625 Ma during the collision of the Nico Pérez Terrane and the Río de la Plata Craton. The shear zone underwent dextral shearing up to 596 Ma under upper to middle amphibolite facies conditions, which was succeeded by sinistral shearing under lower amphibolite to upper greenschist facies conditions until at least 584 Ma. After emplacement of the Cerro Caperuza granite at 570 Ma, the shear zone underwent only cataclastic deformation between the late Ediacaran and the Cambrian. The Sarandí del Yí Shear Zone is thus related to the syncollisional to postcollisional evolution of the amalgamation of the Río de la Plata Craton and the Nico Pérez Terrane. Furthermore, the obtained data reveal that strain partitioning and localization with time, magmatism emplacement, and fluid circulation are key processes affecting the isotopic systems in mylonitic belts, revealing the complexity in assessing the age of deformation of long-lived shear zones.

1. Introduction

Exhumed long-lived shear zones represent fundamental structures that allow studying the coupling between crustal exhumation and strain localization processes as well as the timing at which they take place in the lithosphere. However, assessing the age of the deformation is not a simple task, due to the overprinting caused by the youngest events that may reset the isotopic systems that are used as thermochronometers. It is even more complex to integrate geochronological with macrostructural and microstructural data as well as kinematics in order to create a robust model of the tectonometamorphic evolution of the shear zones, which can further constrain the evolution at the orogen scale.

Several methods can be applied to study the temperature-time (*T-t*) paths of metamorphic rocks, which are based on closure temperatures of isotopic geochronometers (Table 1) [Dodson, 1973; Villa, 1998]. The most widespread methods to constrain the age of the deformation in shear zones consist in either dating synkinematic intrusions or minerals that were formed during mylonitization or constraining the *T-t* paths of adjacent blocks [van der Pluijm *et al.*, 1994]. All these methods, though potentially powerful, have some limitations. Dating synkinematic intrusions represents an indirect and interpretative method [van der Pluijm *et al.*, 1994], whereas dating minerals in the mylonites themselves may be limited by the problem of whether these ages represent neocrystallization or cooling ages [Dunlap, 1997; Mulch and Cosca, 2004]. On the other hand, establishing *T-t* paths of neighboring blocks may be helpful but nevertheless indirect and, in many cases, difficult to obtain due to the lack of equivalent datable mineral associations on both sides of the shear zones.

The Neoproterozoic Brasiliano-Pan-African Orogeny is ubiquitous in eastern South America and western Africa and represents a protracted amalgamation of major crustal blocks along several mobile belts, giving

Table 1. Closure Temperature (T_c) for Different Isotopic Systems

System	T_c (°C)	References
U-Th-Pb zircon	>900	<i>Dahl [1997] and Cherniak and Watson [2000]</i>
U-Th-Pb monazite	>750	<i>Heaman and Parrish [1991]</i>
U-Pb xenotime	>650	<i>Heaman and Parrish [1991]</i>
U-Th-Pb allanite	650	<i>Heaman and Parrish [1991]</i>
U-Th-Pb titanite	650 ± 50	<i>Cherniak [1993], Dahl [1997], and Frost et al. [2000]</i>
U-Pb rutile	620 ± 20	<i>Cherniak [2000], Vry and Baker [2006], and Kooijman et al. [2010]</i>
Sm-Nd garnet	600 ± 30	<i>Mezger et al. [1992]</i>
Rb-Sr muscovite	500 ± 50	<i>Jäger et al. [1967] and Jäger [1977]</i>
K-Ar hornblende	530 ± 40	<i>Harrison [1981]</i>
U-Pb Apatite	425–500	<i>Dahl [1997] and Chamberlain and Bowring [2000]</i>
K-Ar muscovite	350–425	<i>Purdy and Jäger [1976] and Harrison et al. [2009]</i>
Rb-Sr biotite	350	<i>Jenkin [1997]</i>
K-Ar biotite	310 ± 40	<i>Harrison et al. [1985]</i>

rise to the accretion of Gondwana after Rodinia breakup [Almeida et al., 1973; Brito Neves et al., 1999; Cordani et al., 2003; Kröner and Stern, 2004]. Particularly, the juxtaposition of the Río de la Plata, Kalahari, and Congo Cratons together with other continental fragments such as the Nico Pérez Terrane took place in western Gondwana (Figure 1) [Basei et al., 2005; Goscombe et al., 2005; Gray et al., 2008; Foster et al., 2009; Frimmel et al., 2011; Oyhantçabal et al., 2011a, 2011b; Rapela et al., 2011]. Within this framework, the Sarandí del Yí Shear Zone separates the Río de la Plata Craton from the Nico Pérez Terrane (Figure 1), and it thus represents a key element to understand the amalgamation of these crustal segments.

Based on new geochronological and isotopic data from the mylonites of the Sarandí del Yí Shear Zone, this work provides constraints on the tectonothermal evolution of this crustal-scale structure. Furthermore, this information is combined with available kinematic, structural, and microstructural data of the shear zone as well as with geochronological data from the adjacent blocks to present a tectonic model for this part of western Gondwana.

2. Geological Setting

The Sarandí del Yí Shear Zone is a crustal-scale shear zone that constitutes the eastern boundary of the Río de la Plata Craton, which is represented by the Piedra Alta Terrane in Uruguay (Figures 1 and 2) [Oyhantçabal et al., 2011a; Rapela et al., 2011]. The Nico Pérez Terrane and the Neoproterozoic Dom Feliciano Belt are located to the east. The Nico Pérez Terrane includes the Isla Cristalina de Rivera in northern Uruguay and the Taquembó block in southern Brazil, whereas the Dom Feliciano Belt can be further traced to southeastern Brazil (Figure 1) [Fragoso Cesar, 1991; Basei et al., 2005, 2008; Oyhantçabal et al., 2011a].

The Piedra Alta Terrane is constituted by gneisses and granitoids with ages between 2.2 and 2.0 Ga [Oyhantçabal et al., 2011a], which are intruded by the 1.7 Ga old Florida doleritic dyke swarm [Teixeira et al., 1999, 2013]. Paleoproterozoic low- to medium-grade schist belts are recognizable as well [Oyhantçabal et al., 2011a]. Except for the La Paz granite (587.1 ± 7.9 Ma, U-Pb laser ablation-inductively coupled plasma-mass spectrometry zircon) [Cingolani et al., 2012], no Neoproterozoic magmatism is distinguishable in the Piedra Alta Terrane.

The basement of the Nico Pérez Terrane is made up of the Pavas Block, the Valentines-Rivera Granulitic Complex, and the Campanero Unit. The Pavas Block comprises Archean orthogneisses and metasediments [Preciozzi et al., 1979; Hartmann et al., 2001], whereas the Valentines-Rivera Granulitic Complex is constituted by 2.2–2.1 Ga granulitic orthogneisses [Oyhantçabal et al., 2011a, 2012], which are intruded in the west by the 1.7 Ga Illescas rapakivi granite [Campal and Schipilov, 1995]. The Campanero Unit comprises migmatites, amphibolites, banded iron formations, micaschists, and gneisses with zircon ages of 1.7 Ga (Figure 2) [Sánchez Bettucci et al., 2003, 2004; Oyhantçabal, 2005; Mallmann et al., 2007]. Likewise, the Nico Pérez Terrane shows a significant Neoproterozoic reworking that is related to the evolution of the Dom Feliciano Belt. Several Neoproterozoic intrusions can be recognized [Hartmann et al., 2002; Gaucher et al., 2008; Oyhantçabal et al., 2009a, 2012; Gaucher et al., 2014]. Furthermore, Neoproterozoic metasediments and shear zones are also present [Basei et al., 2008; Oyhantçabal et al., 2011a, 2012].

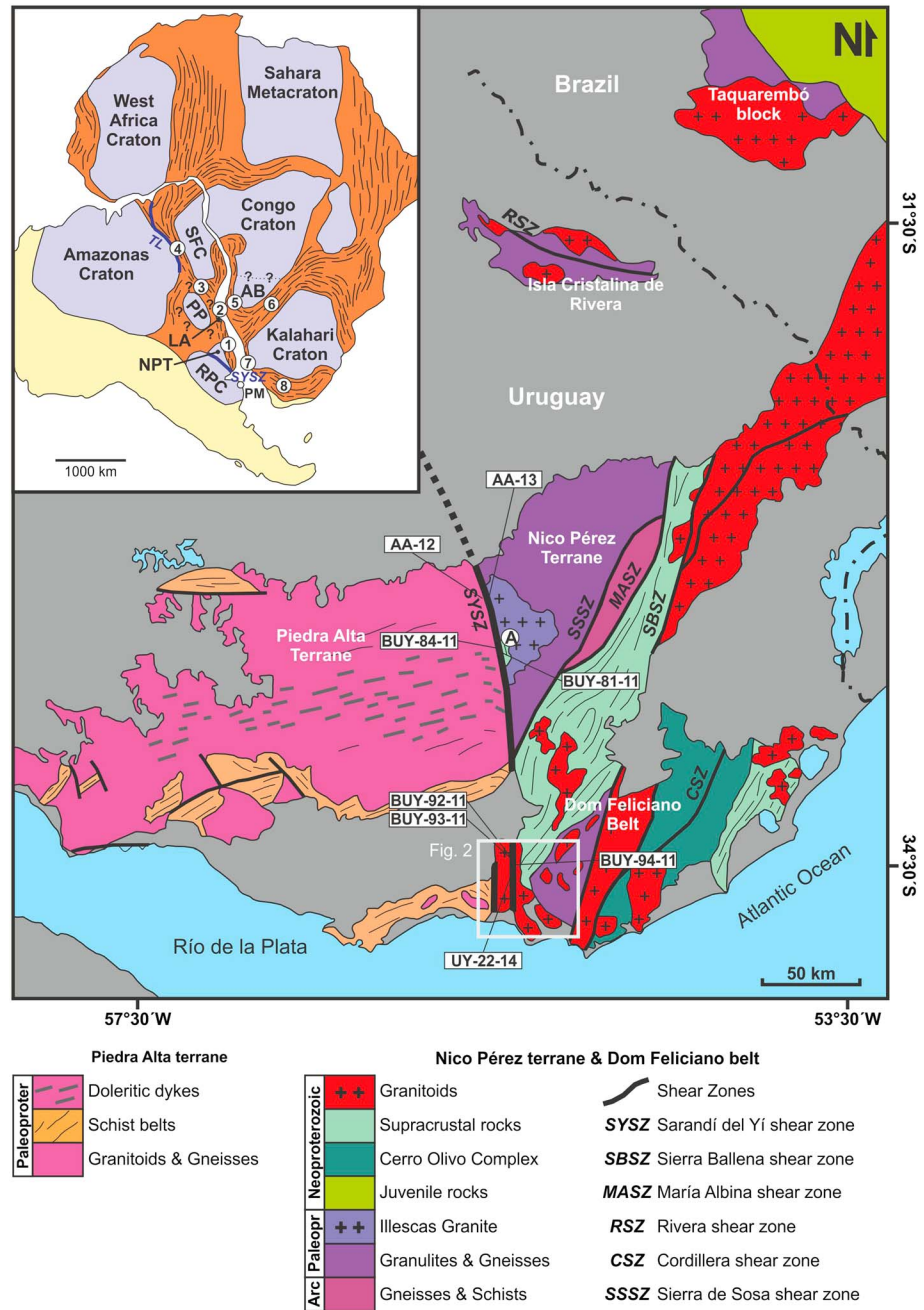


Figure 1. Geological map of the Precambrian of Uruguay modified after *Oyhantçabal et al.* [2011a and references therein]. The inset shows the distribution of main crustal fragments and Neoproterozoic orogenic belts in South America and Africa, modified after *Gray et al.* [2008]. NPT: Nico Pérez Terrane, PP: Paranapanema Block, SFC: São Francisco Craton, RPC: Río de la Plata Craton, AB: Angola Block, and TL: Transbrasiliiano Lineament. 1: Dom Feliciano Belt, 2: Ribeira Belt, 3: Brasília Belt, 4: Araçuaí Belt, 5: Kaoko Belt, 6: Damara Belt, 7: Gariep Belt, and 8: Saldania Belt. The location of the Punta Mogotes borehole (PM), which represents the southeastern margin of the Río de la Plata Craton, is also indicated [*Rapela et al.*, 2011]. The location of the outcrops of the Cerros San Francisco and the Cerro Victoria formations (A) that are near the shear zone and sample locations are shown as well.

The Sarandí del Yí Shear Zone was defined as a structural lineament by *Preciozzi et al.* [1979] and was interpreted afterward as a terrane boundary by *Bossi and Campal* [1992]. *Oyhantçabal et al.* [1993] considered it as a pre-Brasiliano dextral shear zone that was sinistrally reactivated during the late Neoproterozoic. Later, *Oyhantçabal et al.* [2011a] proposed it as the eastern margin of the Río de la Plata Craton. On the basis of

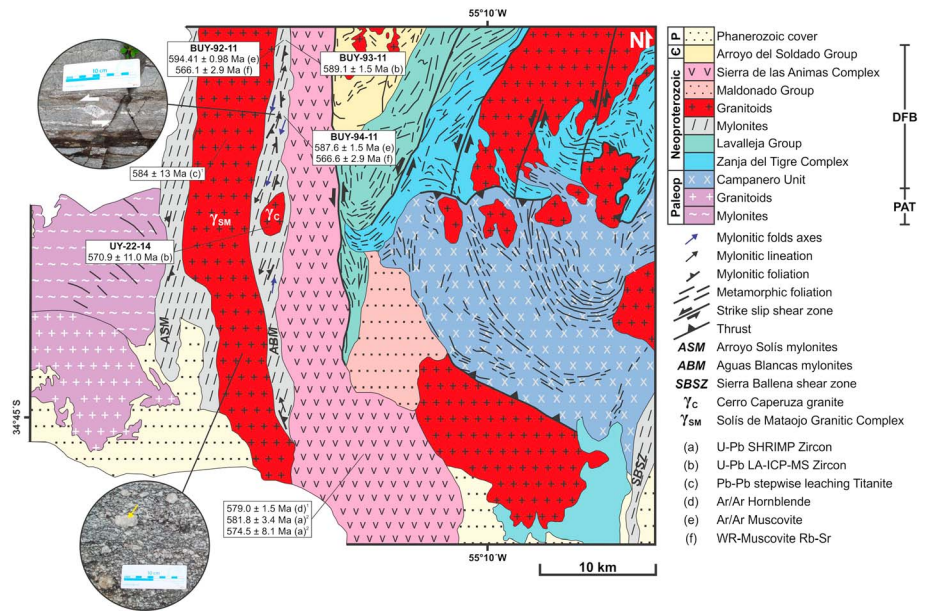


Figure 2. Geological map of the southernmost Sarandí del Yí Shear Zone and adjacent blocks (modified after *Oyhantçabal et al.* [2001, 2005] and *Spoturno et al.* [2011, 2012]). The shear zone includes the Aguas Blancas and Arroyo Solís mylonites. Field photographs show sinistral σ -type feldspar mantled porphyroclasts with recrystallized tails in the mylonites and magmatic foliation defined by shape-preferred orientation of euhedral K feldspar megacrysts (arrow) in the Solís de Mataojo Granitic Complex. New and available geochronological data of key units are indicated as well (1: *Oyhantçabal et al.* [2007] and 2: *Rapalini et al.* [2015]). DFB: Dom Feliciano Belt and PAT: Piedra Alta Terrane. In the Dom Feliciano Belt, metavolcano-sedimentary (Zanja del Tigre Complex, Lavalleja Group, and Maldonado Group) and metasedimentary (Arroyo del Soldado Group) sequences are shown as well.

structural, microstructural, and kinematic data, *Oriolo et al.* [2015] determined that deformation in the Sarandí del Yí Shear Zone started under middle amphibolite to upper amphibolite facies conditions with dextral shearing in the easternmost Piedra Alta Terrane during juxtaposition of the Río de la Plata Craton and the Nico Pérez Terrane. Subsequent lower amphibolite to upper greenschist facies metamorphism was related to pure shear-dominated sinistral shearing, which was accompanied by contemporaneous magmatism, and was followed by a late cataclasis that reworked the easternmost border of the shear zone [*Oriolo et al.*, 2015].

Though the sinistral shearing is considered to be Neoproterozoic in age due to the emplacement of the syn-kinematic calc-alkaline Solís de Mataojo Granitic Complex (Figure 2; 580 ± 15 Ma, Rb-Sr whole rock; 584 ± 13 Ma, single-phase Pb-Pb stepwise leaching titanite) [*Umpierre and Halpern*, 1971; *Oyhantçabal et al.*, 2007], the timing of the dextral shearing is not well constrained. This first event took place prior to the Neoproterozoic sinistral shearing and also postdates the emplacement of the 1.7 Ga old Florida doleritic dyke swarm [*Teixeira et al.*, 1999, 2013], as these dykes are dextrally sheared toward the shear zone [*Oyhantçabal et al.*, 1993; *Oriolo et al.*, 2015]. Therefore, the onset of the deformation during accretion of the Nico Pérez Terrane to the eastern margin of the Río de la Plata Craton could be placed at any time between the late Paleoproterozoic (<1.7 Ga) and the late Neoproterozoic.

3. Sample Description

Samples AA-13, BUY-81-11, BUY-84-11, BUY-92-11, BUY-93-11, and BUY-94-11 were collected from mylonites of the Sarandí del Yí Shear Zone itself (Figure 1). On the other hand, AA-12 corresponds to a granitic mylonite located in the easternmost Piedra Alta Terrane, which was deformed during dextral shearing along the shear zone. A sample (UY-22-14) from the Cerro Caperuza granite was obtained as well (Figure 2), as it intrudes the shear zone and shows no significant ductile deformation, thus providing a constraint on the end of the mylonitization. Sample locations and applied methods are presented in Table S1 in the supporting information, whereas analytical procedures are described in supporting information S1.

The sample AA-12 corresponds to a mylonite made up of quartz, K feldspar, plagioclase, hornblende, and biotite. Quartz shows interlobate grain boundaries, leftover grains, and minor chessboard extinction, which accounts for grain boundary migration recrystallization at temperatures above approximately 600°C [Kruhl, 1996; Stipp *et al.*, 2002]. Feldspars exhibit local recrystallization along the edge of the grains, indicating recrystallization temperatures above 550°C [Voll, 1976; Pryer, 1993]. Biotite and hornblende are preferentially oriented in two planes that define the S and C' of dextral shear bands, which are also observable at mesoscale. Hornblende crystals are typically euhedral and present only minor fracturing (Figure 3a) [Oriolo *et al.*, 2015].

The sample AA-13 from a granitic mylonite is made up of quartz, K feldspar, and plagioclase. S-C' shear bands and feldspar σ -type mantled porphyroblast microstructures indicate sinistral shearing (Figure 3b). Sutured grain boundaries point to grain boundary migration recrystallization in quartz, although minor evidences of subgrain rotation recrystallization can be recognized as well, indicating recrystallization temperatures of 450–550°C [Stipp *et al.*, 2002]. Feldspars develop core and mantle structures, with occasionally antbookshelf structures, indicating temperatures of 450–550°C [Passchier and Trouw, 2005, and references therein]. Scarce sericite and epidote are also present along shear band planes.

The mylonite of the sample BUY-81-11 is constituted by quartz, K feldspar, plagioclase, and hornblende. Sutured grain boundaries point to grain boundary migration recrystallization at approximately 500–550°C for quartz [Stipp *et al.*, 2002]. Core and mantle structures in feldspars reveal sinistral shearing both at mesoscale and microscale and point to recrystallization temperatures of 450–550°C [Passchier and Trouw, 2005, and references therein]. Hornblende crystals present significant fracturing and are sometimes boudinaged parallel to the stretching lineation direction (Figure 3c).

The sample BUY-84-11 is an ultramylonite constituted by quartz, feldspar, and sericite. Quartz crystals form aggregates with foam textures indicating recovery. Core and mantle structures in feldspars show sinistral shearing and point to recrystallization temperatures of 450–550°C [Passchier and Trouw, 2005, and references therein]. Pressure solution is revealed by the presence of opaque minerals-rich solution seams.

UY-22-14 corresponds to the Cerro Caperuza granite, which presents equigranular texture and is constituted by quartz, K feldspar, plagioclase, and scarce biotite (Figure 3d).

The deformed porphyritic felsic intrusion of the sample BUY-93-11 is made up of quartz and feldspar. Sutured grain boundaries point to grain boundary migration recrystallization at approximately 500–550°C for quartz [Stipp *et al.*, 2002]. Core and mantle structures in feldspars reveal sinistral shearing and recrystallization temperatures of 450–550°C [Passchier and Trouw, 2005, and references therein].

Both BUY-92-11 and BUY-94-11 correspond to mylonites, which are constituted by quartz, K feldspar, plagioclase, and muscovite. Sinistral shearing is indicated by S-C' shear bands, σ -type feldspar mantled porphyroblasts with asymmetric myrmekites, mica fish, and oblique foliation of elongated quartz grains. S-C' shear bands and σ -type feldspar mantled porphyroblasts are also observable at mesoscale. Sutured grain boundaries point to grain boundary migration recrystallization in quartz and recrystallization temperatures of 500–550°C (Figure 3e) [Stipp *et al.*, 2002]. Feldspars develop core and mantle structures, which are sometimes accompanied by microshear zones that show internal recrystallization, indicating temperatures of 450–550°C [Passchier and Trouw, 2005, and references therein]. Muscovite typically develops mica fish microstructures and is oriented parallel to the S or C' planes of the shear bands in the mylonites (Figure 3f), suggesting that they are synkinematic minerals. This interpretation is further supported by the lack of muscovite in the protolith of the mylonites, i.e., the Solís de Matajojo Granitic Complex. Locally, solution seams parallel to shear band planes can be recognized as well. They are made up of fine-grained aggregates of biotite and opaque minerals.

4. Results

4.1. U-Pb Ages and Hf Isotopes

Zircons from the sample AA-12 are typically prismatic to equant and show oscillatory zoning, sometimes with homogeneous bright cores (Figure 4a). A concordant age of 596.0 ± 3.3 Ma was obtained considering 15 out of 24 spots (Figure 5a, data points with low correlation coefficients rejected), which is interpreted as the crystallization age of the magmatic protolith.

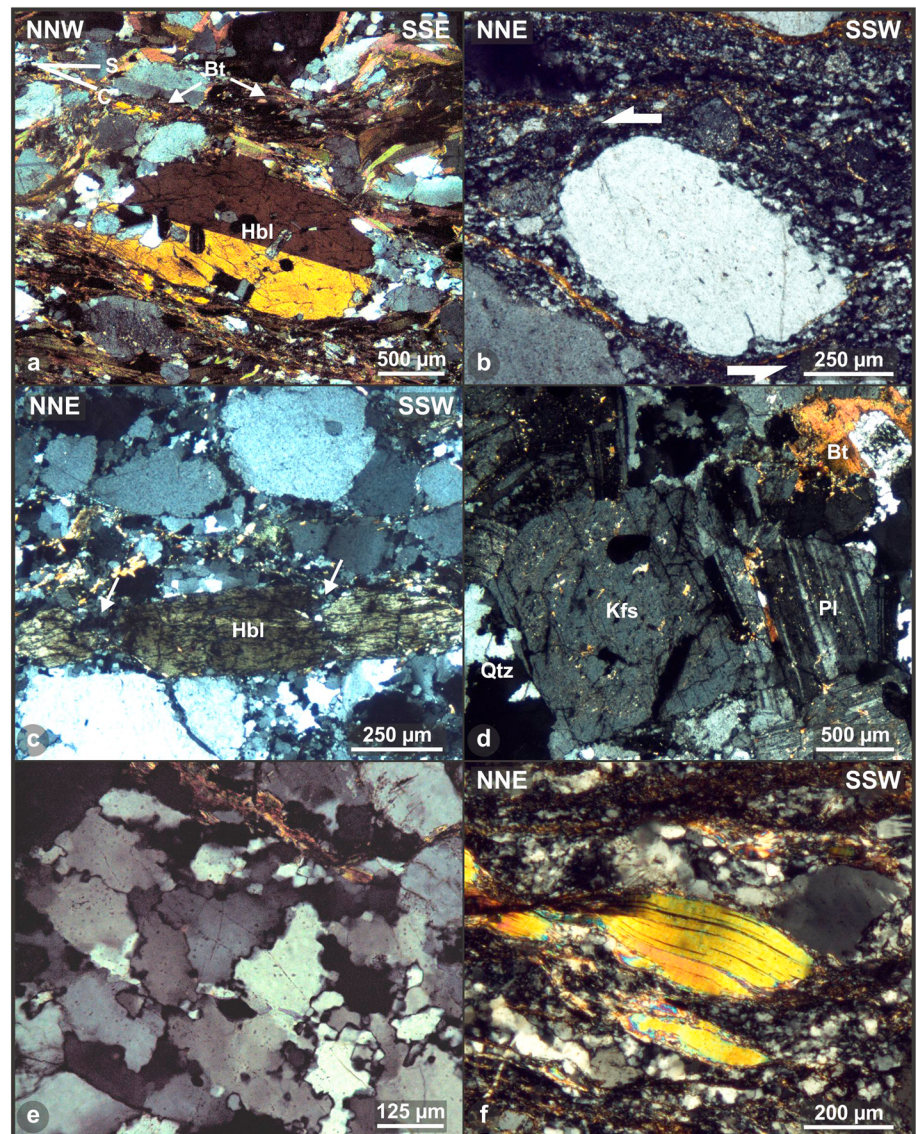


Figure 3. Photomicrographs of microstructures from the analyzed samples (cross-polarized light). (a) Dextral S-C' shear band with shape-preferred orientation of biotite and hornblende (AA-12, XZ section) [Oriolo *et al.*, 2015]. (b) Sinistral σ -type mantled porphyroblast of feldspar (AA-13, XZ section). (c) Boudinage of hornblende parallel to the stretching lineation direction (XZ section). Arrows indicate interboudin areas (BUY-81-11). (d) Equigranular texture of the Cerro Caperuza granite formed by euhedral feldspar crystals (UY-22-14). (e) Sutured quartz crystals showing grain boundary migration (BUY-94-11) [Oriolo *et al.*, 2015]. (f) Mica fish microstructure in muscovite (BUY-94-11, XZ section).

In the case of AA-13, zircons present oscillatory zoning as well as homogeneous dark or bright cores (Figure 4b). A 2048.3 ± 11.0 Ma concordia age is interpreted as the age of the crystallization of the magmatic protolith based on 23 out of 26 data points (Figure 5b, discordant data rejected). In addition, Hf model ages (T_{DM}) between 2.20 and 2.47 Ga as well as $\epsilon_{Hf}(t_1)$ between +2.26 and +7.23 were obtained for the zircons (Figure 5c and Table S4 in the supporting information).

Zircons from BUY-81-11 are prismatic and, in some cases, fragmented. Cores are dominantly homogeneous (Figure 4c) and present a weighted mean $^{207}\text{Pb}/^{206}\text{Pb}$ age of 2025 ± 37 Ma (Figure 5d, six spots, discordant data rejected). On the other hand, oscillatory zoning is found in the rims (Figure 4), which show a concordant age of 623.0 ± 5.1 Ma based on 6 out of 15 data points (Figure 5e, data with high U or common ^{206}Pb content rejected).

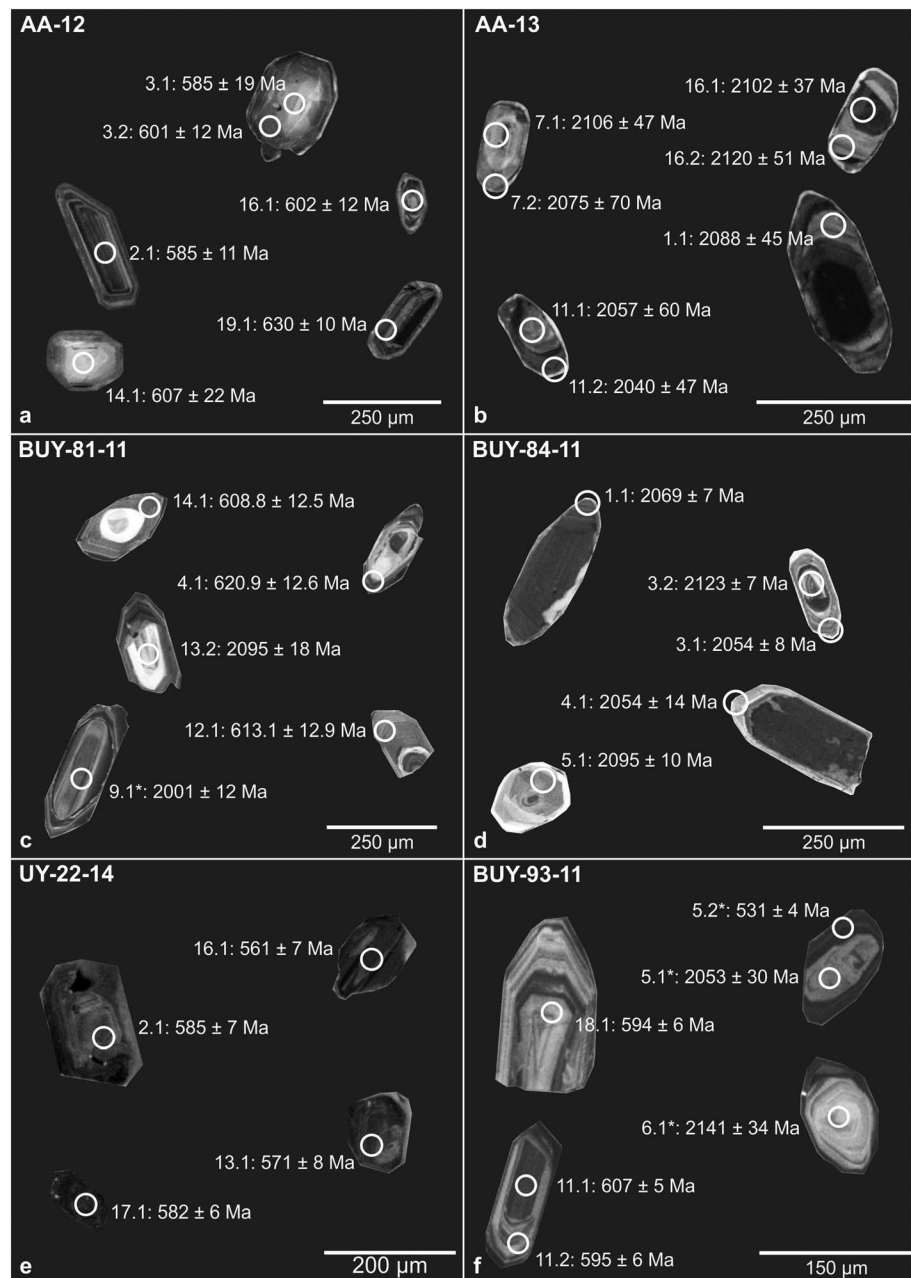


Figure 4. Cathodoluminescence images of representative zircons. Individual U-Pb ages are shown. Asterisk indicates discordant ages.

Zircons from BUY-84-11 are prismatic and occasionally round and exhibit homogeneous dark cores surrounded by overgrowths with oscillatory zoning (Figure 4d). A concordia age of 2068.9 ± 4.2 Ma considering six out of eight spots is interpreted as the crystallization age of the magmatic protolith, which is recorded in both cores and overgrowths (Figure 5f, discordant data rejected).

In the Cerro Caperuza granite (sample UY-22-14), zircons are prismatic with oscillatory zoning and present a concordant age of 570.9 ± 11.0 Ma considering 5 out of 26 data points (Figures 4e and 5g, highly discordant data or with high U or common ^{206}Pb content rejected). Some spots show slightly older concordant ages that may indicate reworking of magmatic zircons with ages between approximately 620–580 Ma (Figure 5g).

Prismatic to slightly rounded zircons with cores that are either homogeneous or zoned were recognized for BUY-93-11. Homogeneous bright cores present a weighted mean $^{207}\text{Pb}/^{206}\text{Pb}$ age of 2115 ± 38 Ma (Figure 5h,

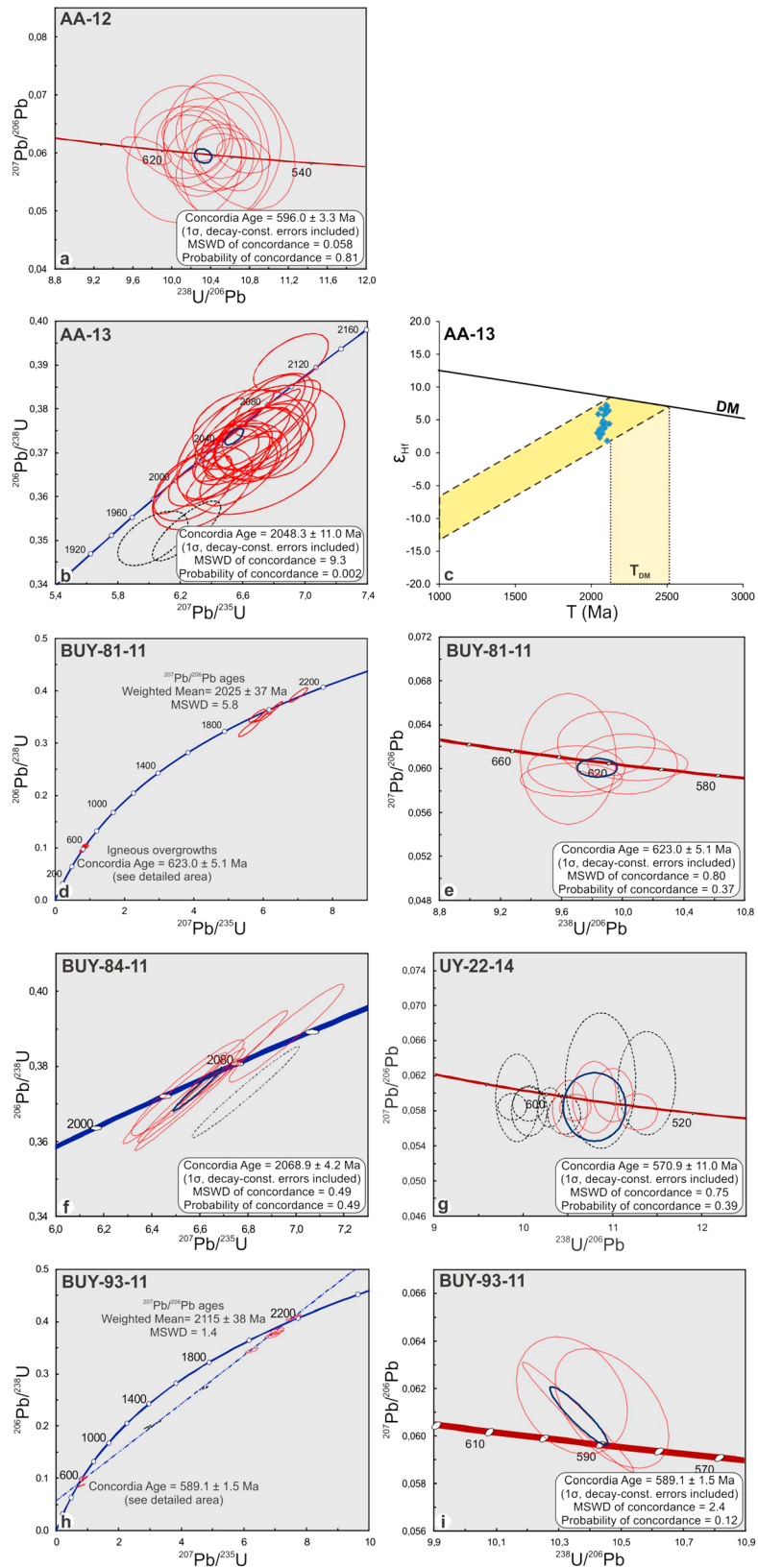


Figure 5. U-Pb diagrams. Red ellipses indicate data used for age calculations, whereas dashed ellipses represent data that were not considered. Errors depicted at the 2 σ level. ϵ_{HF} versus time data from the sample AA-13 are also shown. Analytical procedures are indicated in Text S1, and data results are presented in Table S4 in the supporting information.

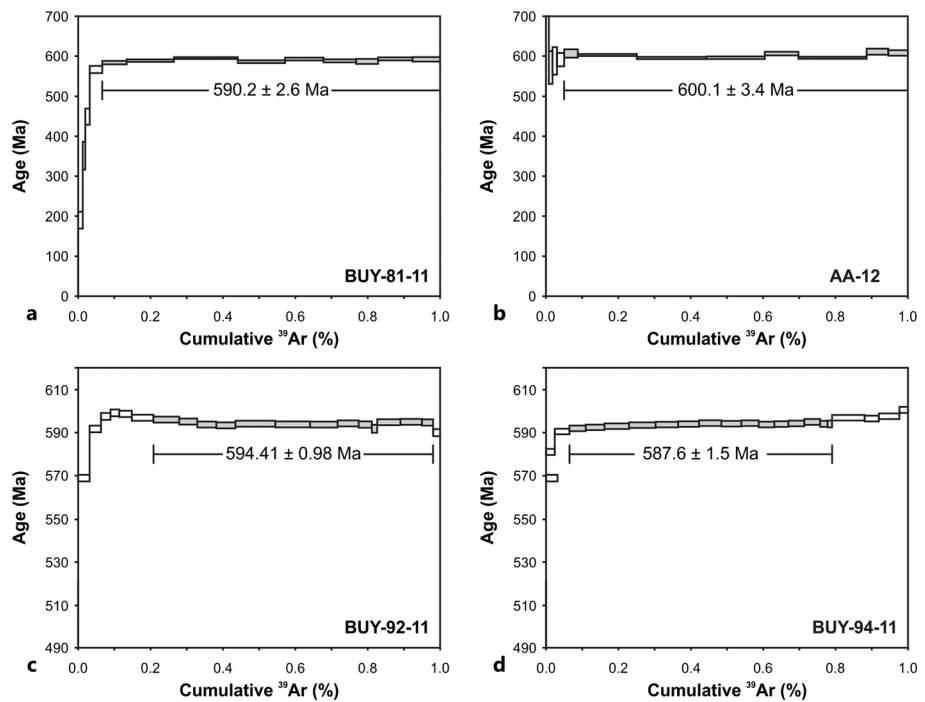


Figure 6. Ar/Ar age spectrum from hornblende and muscovite samples. Plateau steps are colored in grey, whereas rejected steps are indicated in white.

7 out of 26 spots). Three points measured in overgrowths with oscillatory zoning exhibit a concordant age of 589.1 ± 1.5 Ma (Figures 4f and 5i, highly discordant data or with high U or common ^{206}Pb content rejected).

4.2. $^{40}\text{Ar}/^{39}\text{Ar}$

A hornblende plateau age of 600.1 ± 3.4 Ma was obtained for the sample AA-12, whereas the sample BUY-81-11 presents a hornblende plateau age of 590.2 ± 2.6 Ma (Figures 6a and 6b). On the other hand, the white mica concentrates yield plateau ages of 594.41 ± 0.98 Ma and 587.6 ± 1.5 Ma for the samples BUY-92-11 and BUY-94-11, respectively (Figures 6c and 6d).

4.3. Rb-Sr

Two Rb-Sr isochron ages were defined by muscovite and whole rock concentrates from the same muscovite samples that were analyzed using the $^{40}\text{Ar}/^{39}\text{Ar}$ method. The sample BUY-92-11 shows an age of 566.1 ± 2.9 Ma, whereas the sample BUY-94-11 presents an age of 566.6 ± 2.9 Ma (Table S4 in the supporting information).

5. Discussion

5.1. Protolith Petrogenesis

U-Pb zircon data reveal two protoliths generated during the Paleoproterozoic and the Neoproterozoic. However, no significant textural differences are observed between both zircon groups. Zircons are prismatic and occasionally round with oscillatory zoning and $\text{Th}/\text{U} > 0.1$ (Figure 4 and Table S4 in the supporting information), which is indicative of a magmatic origin [Hoskin and Schaltegger, 2003, and references therein]. As deformation conditions along the Sarandí del Yí Shear Zone did not surpass amphibolite facies conditions [Oriolo *et al.*, 2015], the U-Pb zircon ages are interpreted to represent the age of the magmatic protolith rather than a direct age constraint on the deformation along the shear zone.

Two concordant ages of 2048.3 ± 11.0 Ma (sample AA-13) and 2068.9 ± 4.2 Ma (sample BUY-84-11) as well as two $^{207}\text{Pb}/^{206}\text{Pb}$ weighted mean ages of 2025 ± 37 Ma (sample BUY-81-11) and 2115 ± 38 Ma (sample BUY-93-11) provide evidence of a late Rhyacian-early Orosirian magmatic event and are equivalent to ages of granitoids and gneisses of the basement of the Piedra Alta Terrane (Figure 5) [Hartmann *et al.*, 2000; Santos *et al.*, 2003; Peel and Preciozzi, 2006]. Hf isotopes from the zircons of the sample AA-13 yield a T_{DM} age range from 2.20 to

2.47 Ga as well as $\epsilon_{\text{Hf}}(t_1)$ between +2.26 and +7.23 (Figure 5c), which indicates contribution of Paleoproterozoic juvenile continental crust. Hf isotopes from the Cerro Colorado granite (eastern Piedra Alta Terrane) are almost identical (Oriolo et al., submitted manuscript, 2015), and similar Sm-Nd model ages were obtained in different intrusions of the Piedra Alta Terrane as well [Peel and Preciozzi, 2006], thus supporting a crustal affinity of the mylonitic protolith with the Piedra Alta Terrane.

On the other hand, Neoproterozoic concordant ages of 596.0 ± 3.3 Ma (sample AA-12), 623.0 ± 5.1 Ma (sample BUY-81-11), and 589.1 ± 1.5 Ma (sample BUY-93-11) were obtained in three samples (Figure 5). The zircons of AA-12 only yield Neoproterozoic ages, but BUY-81-11 and BUY-93-11 also show inheritance of Paleoproterozoic zircons (Figures 4 and 5 and Table S4 in the supporting information). In addition, Neoproterozoic ages in BUY-81-11 zircons were only detected in overgrowths, whereas BUY-93-11 contains Neoproterozoic neofomed zircons as well (Figure 4). Consequently, obtained Neoproterozoic ages may have resulted from both reequilibration of inherited Paleoproterozoic crystals and neocrystallization in the presence of a melt [Bea et al., 2007; Geisler et al., 2007].

5.2. Tectonothermal Evolution of the Sarandí del Yí Shear Zone

Despite previous works that suggested a Mesoproterozoic age for the onset of the deformation [Bossi and Cingolani, 2009; Gaucher et al., 2011a], new results provide solid evidence of Neoproterozoic nucleation for the Sarandí del Yí Shear Zone (Figure 7a). The only previous constraint for the dextral shearing was the bending of the 1.7 Ga old Florida doleritic dyke swarm, which provides a maximum age for this event. Results obtained for the sample AA-12 indicate dextral shearing up to 596 Ma. Similar zircon and hornblende ages together with hornblende microstructures point to emplacement and fast cooling of this intrusion below approximately 500°C during dextral shearing. Likewise, the oldest concordant age of 623.0 ± 5.1 Ma (sample BUY-81-11) represents a maximum age for magmatism related to deformation along the shear zone. This value is thus interpreted as syncollisional to early postcollisional magmatism related to the amalgamation of the Nico Pérez Terrane and the Río de la Plata Craton along the Sarandí del Yí Shear Zone and supports proposals indicating juxtaposition of both crustal blocks during the Neoproterozoic [Oyhantçabal et al., 2011a; Rapela et al., 2011]. As this sample shows evidence of sinistral shearing at temperatures of 450–550°C, which are similar to the closure temperature for amphibole, the significantly younger $^{40}\text{Ar}/^{39}\text{Ar}$ plateau age of 590.2 ± 2.6 Ma from strongly deformed hornblende crystals may indicate reworking of these rocks and resetting of the K/Ar system at approximately 590 Ma. This is also supported by structural evidence indicating progressive strain localization toward the east [Oriolo et al., 2015].

The subsequent sinistral movement was previously constrained by the age of the synkinematic Solís de Matajojo Granitic Complex (Figure 2) [Oyhantçabal et al., 2001, 2007]. The U-Pb sensitive high-resolution ion microprobe (SHRIMP) concordant age of 589.1 ± 1.5 Ma of the sample BUY-93-11 together with the $^{40}\text{Ar}/^{39}\text{Ar}$ hornblende plateau age of 590.2 ± 2.6 Ma of sinistraly sheared mylonites and $^{40}\text{Ar}/^{39}\text{Ar}$ plateau ages of 594.41 ± 0.98 Ma and 587.6 ± 1.5 Ma of synkinematic muscovites constrains the sinistral shearing at ~594–584 Ma. As temperature conditions for the sinistral shearing are constrained at 450–550°C [Oriolo et al., 2015], which are above the closure temperature of the K/Ar system for muscovites, muscovite ages probably reflect cooling after synkinematic crystallization [Mulch and Cosca, 2004; Rolland et al., 2008].

Rb-Sr data are significantly younger than the respective $^{40}\text{Ar}/^{39}\text{Ar}$ muscovite ages. As the latter match other geochronological data as well as geological evidences (e.g., intrusion of the Cerro Caperuza granite postdating the ductile deformation along the shear zone), Rb-Sr data may not reflect true cooling stories [Jenkin, 1997]. As indicated by Eberlei et al. [2015], deformation strongly affects the Rb-Sr geochronometer at <500°C. Likewise, Bozkurt et al. [2011] demonstrated that fluid-assisted deformation under cataclastic conditions may reopen this isotopic system. Local cataclastic reworking, pressure solution, and associated fluid circulation are recorded in the mylonites [Oriolo et al., 2015], which could account for reequilibration of the Rb-Sr system during low-temperature fluid-assisted deformation. However, $^{40}\text{Ar}/^{39}\text{Ar}$ muscovite ages seem to remain unaffected by these processes, which may suggest that Sr presents an unlikely more effective diffusivity than Ar under similar conditions. Alternatively, a more plausible explanation could be that the Rb-Sr system has remained closed for the muscovites but was affected for the whole rock system, giving rise to whole rock-muscovite isochron ages that are younger than expected.

On the basis of hornblende and muscovite geochronological data, cooling rates can be estimated for the Sarandí del Yí Shear Zone (Figure 7b). $^{40}\text{Ar}/^{39}\text{Ar}$ hornblende and muscovite data reveals a cooling rate of

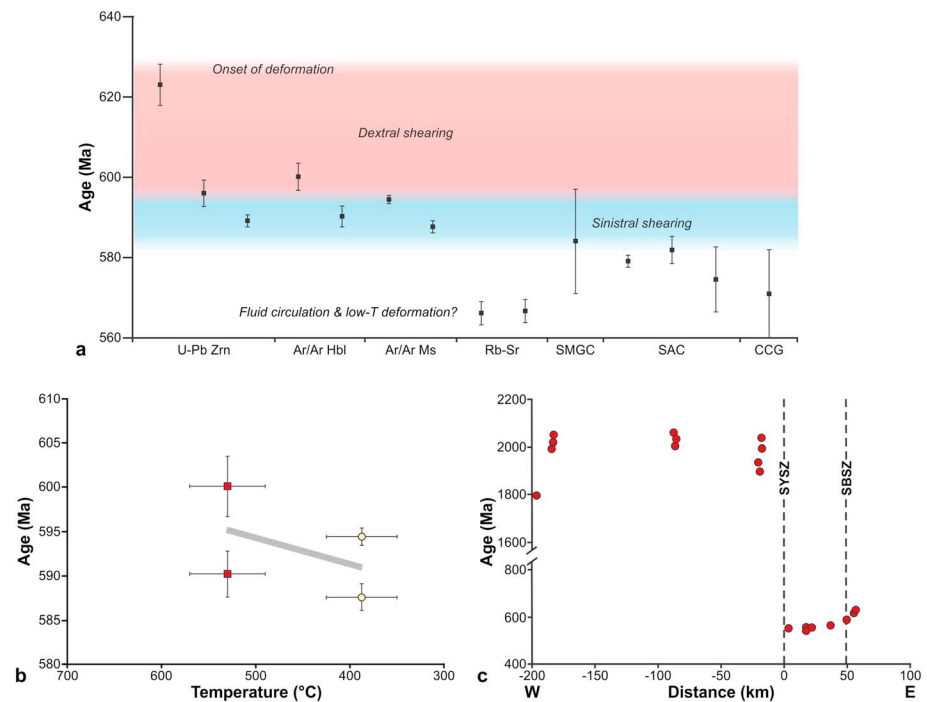


Figure 7. (a) Summary of the geochronological data from the Sarandí del Yí Shear Zone. Ages of associated intrusions are also shown (SMGC: Solís de Mataojo Granitic Complex [Oyhantçabal et al., 2007], SAC: Sierra de las Ánimas Complex [Oyhantçabal et al., 2007; Rapalini et al., 2015], and CCG: Cerro Caperuza granite, this work). The age of the dextral (red) and the sinistral shearing (blue) are indicated as well. (b) t versus T plots based on hornblende (red squares) and muscovite (yellow circles) data with average cooling path. Closure temperatures after references from Table 1. (c) West-east K-Ar muscovite profile across the Piedra Alta Terrane, the Nico Pérez Terrane, and the Dom Feliciano Belt, modified after Oyhantçabal et al. [2011a]. The position of the Sarandí del Yí Shear Zone (SYSZ) and the Sierra Ballena Shear Zone (SBSZ) is presented.

approximately $34^{\circ}\text{C Ma}^{-1}$ between $\sim 595\text{--}590$ Ma (Figure 7b). On the other hand, the cooling rate of $34^{\circ}\text{C Ma}^{-1}$ may have resulted from fast exhumation during sinistral shearing. Vertical extrusion related to pure shear-dominated deformation along the Sarandí del Yí Shear Zone could account for this process [Oriolo et al., 2015]. Comparable cooling rates related to shearing and rapid exhumation were also reported from the Carthage-Colton Mylonite Zone of the Adirondack Mountains [Bonamici et al., 2014].

Nevertheless, the estimated cooling rates have to be considered carefully due to the complexity of the processes involved in the shearing. Particularly, the existence of several intrusions during deformation appears to be one of the most significant processes affecting the isotopic systems, as the existence of magmatism resets the chronometers and true cooling paths cannot be calculated (Figure 7a). In addition, strain localization during exhumation of the shear zone also induces local reworking of the mylonitic belt and consequent reset of the thermochronometers [Mulch et al., 2006]. Comparison of hornblende data from the dextrally and sinistrally sheared domains shows younger ages in the latter, supporting progressive strain localization toward the east inferred from structural data [Oriolo et al., 2015]. Consequently, recrystallization-related processes such as strain and fluids as well as magmatism play a major role in the closure of isotopic systems in mylonites, being temperature not the only significant variable, as outlined by Villa [1998].

The age of 570.9 ± 11 Ma for the Cerro Caperuza granite together with the age of the alkaline plutonic-volcanic Sierra de las Ánimas Complex (Figure 2; 579 ± 1.5 Ma, Ar/Ar hornblende; 581.8 ± 3.4 Ma, 574.5 ± 8.1 Ma, U-Pb SHRIMP zircon) [Oyhantçabal et al., 2007; Rapalini et al., 2015] provides a solid constraint for the end of the ductile deformation in the shear zone (Figure 7a). Likewise, the Rb-Sr ages of the mylonites can be interpreted as the result of the reequilibration of the Rb-Sr isotopic system due to fluid circulation, probably associated with low-temperature deformation that is recognizable in both mylonites and the

Cerro Caperuza granite [Oriolo et al., 2015]. It can be thus inferred that cataclastic deformation in the easternmost shear zone started after 570 Ma. Moreover, the Cerros San Francisco and the Cerro Victoria formations are folded and affected by low-*T* shear zones and faults near the cataclasites of the Sarandí del Yí Shear Zone in the western Nico Pérez Terrane (Figure 1) [Montaña and Sprechmann, 1993; Oriolo et al., 2015]. As they did not achieve metamorphic conditions higher than lower greenschist facies [Gaucher, 2000; Blanco et al., 2009; Sánchez Bettucci et al., 2010] and present a late Ediacaran-early Cambrian age [Blanco et al., 2009; Gaucher et al., 2011b], deformation of these sequences may be related to late Ediacaran-Cambrian cataclastic deformation along the shear zone. Furthermore, Rapalini and Sánchez Bettucci [2008] interpreted a postfolding remagnetization event in the Cerro Victoria Formation as evidence for an Early Cambrian event. Consequently, brittle deformation in the Sarandí del Yí Shear Zone can be characterized as a long-term process that took place between the late Ediacaran and the Cambrian.

5.3. Implications for Western Gondwana

Recent contributions outlined the allochthony of the Nico Pérez Terrane regarding the Río de la Plata Craton and its African origin [Oyhantçabal et al., 2011a; Rapela et al., 2011], which seems to be particularly related to the Congo Craton (Oriolo et al., submitted manuscript, 2015). Rapela et al. [2011] also indicated that not only the Nico Pérez but also other South American crustal blocks such as the Mar del Plata and Encantadas terranes represent African remnants that were accreted during the Brasiliano-Pan-African Orogeny.

On the other hand, the oldest Neoproterozoic record in the southern Dom Feliciano Belt is constituted by the high-grade rocks of the Cerro Olivo Complex, which contains zircons yielding U-Pb SHRIMP concordant ages of ~750–800 Ma [Hartmann et al., 2002; Oyhantçabal et al., 2009a; Basei et al., 2011a; Lenz et al., 2011]. Due to similar ages reported in the Coastal Terrane of the Kaoko Belt [Kröner et al., 2004; Konopásek et al., 2008], both regions were correlated and these ages were interpreted as the timing of rifting-related magmatism during the Rodinia breakup [Kröner et al., 2004; Oyhantçabal et al., 2009a; Basei et al., 2011a; Frimmel et al., 2011; Rapela et al., 2011; Konopásek et al., 2014]. Likewise, high-grade metamorphism is also recorded in both the Cerro Olivo Complex and the Coastal Terrane. Zircon overgrowths yielding ages of 641 ± 17 Ma [Oyhantçabal et al., 2009a] and 654 ± 3 Ma [Lenz et al., 2011] as well as U-Pb Isotope Dilution Thermal Ionization Mass Spectrometry monazite ages of 645 ± 4 [Basei et al., 2011a] were reported for gneisses of the Cerro Olivo Complex. On the other hand, magmatism at approximately 650 Ma [Seth et al., 1998] and several ages between approximately 660 and 625 Ma were obtained in the Coastal Terrane [Goscombe et al., 2005; Konopásek et al., 2008] and were interpreted as the age of high-grade metamorphism and migmatization [Goscombe and Gray, 2007; Konopásek et al., 2008].

The onset of deformation along the Sarandí del Yí Shear Zone at 630–625 Ma constrains the age of the amalgamation of the Nico Pérez Terrane and the Río de la Plata Craton. These results support models from Oyhantçabal et al. [2011a] and Rapela et al. [2011] considering juxtaposition of both crustal blocks during the Neoproterozoic, previously constrained by the 584 ± 13 Ma age of the Solís de Mataojo Granitic Complex [Rapela et al., 2011]. Contrasting cooling age patterns on both sides of the shear zone reinforce this interpretation (Figure 7c) [Oyhantçabal et al., 2011a]. Consequently, metamorphic conditions of the Cerro Olivo Complex [Lenz et al., 2011] could be explained by arc-related high-grade metamorphism and magmatism followed by the accretion of the Nico Pérez Terrane and the Río de la Plata Craton (Figures 8a and 8b). Similar *P-T* conditions in arc settings were reported by Tibaldi et al. [2013] and Maki et al. [2014] in the Famatinian arc (western Sierras Pampeanas) and the Higo metamorphic terrane (central Kyushu), respectively. Likewise, Basei et al. [2011a] interpreted a collisional event at 635 ± 10 Ma in the Cerro Olivo Complex. Muscovite K-Ar ages between 630 and 620 Ma [Oyhantçabal et al., 2007] in the Cerro Olivo Complex as well as an approximately 630 Ma rutile metamorphic age in metabasalts from the Dom Feliciano Belt in Uruguay [Sánchez Bettucci et al., 2003] provide further constraints for the age of exhumation and metamorphism related to the accretion. This also agrees with interpretations indicating an arc/back-arc domain at the attenuated Congo Craton margin at ~650–630 Ma [Goscombe and Gray, 2007, 2008; Konopásek et al., 2014] and the age of the docking of the Coastal Terrane to the Kaoko Belt, which must have occurred after 645 Ma but prior to 580 Ma according to Goscombe and Gray [2007]. In Brazil, Gross et al. [2006] obtained Sm-Nd whole rock garnet ages between ~660 and 600 Ma in the Paleoproterozoic basement of the Dom Feliciano Belt, whereas the collisional event in the belt has been placed between approximately 650 and 600 Ma [Basei et al., 2008, 2011b; Florisbal et al., 2012; Philipp et al., 2013].

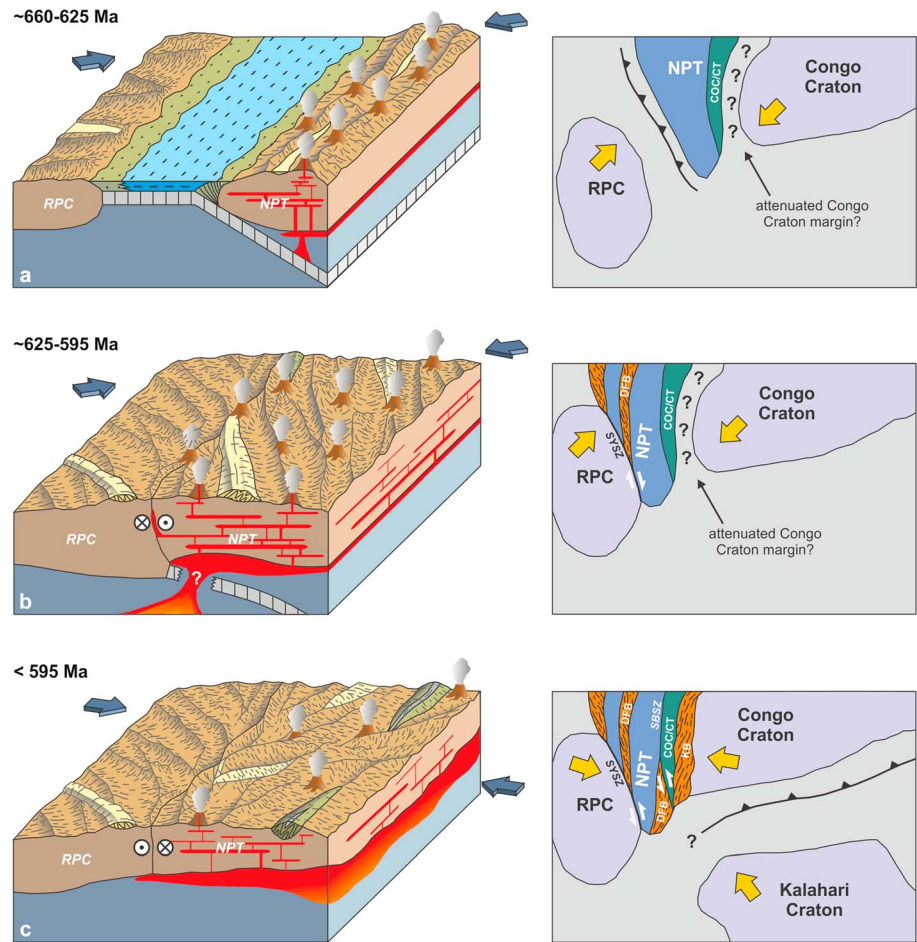


Figure 8. Tectonic evolution model for the Sarandí del Yí Shear Zone and adjacent crustal blocks. The paleogeographic framework is schematized on the right. RPC: Río de la Plata Craton, NPT: Nico Pérez Terrane, COC/CT: Cerro Olivo Complex/Coastal Terrane, DFB: Dom Feliciano Belt, KB: Kaoko Belt, SYSZ: Sarandí del Yí Shear Zone, and SBSZ: Sierra Ballena Shear Zone. (a) Subduction under the Nico Pérez Terrane, which was probably part of the attenuated margin of the Congo Craton. (b) Juxtaposition of the Río de la Plata Craton and the Nico Pérez Terrane and consequent onset of deformation along the Sarandí del Yí Shear Zone at 630–625 Ma. During the postcollisional phase and associated slab break off, dextral shearing along the shear zone was coeval with deformation, metamorphism, and magmatism in the Dom Feliciano Belt. (c) Sinistral shearing in the Sarandí del Yí Shear Zone at 594–584 Ma. Further postcollisional magmatism and sinistral shearing along the shear zones of the Dom Feliciano Belt as well as back-arc extension are recorded. The switch to sinistral shearing could be related to the onset of the convergence of the Kalahari Craton.

Widespread postcollisional magmatism is recorded in the Nico Pérez Terrane and the Dom Feliciano Belt after approximately 620 Ma [Oyhantçabal et al., 2007; Lara et al., 2013]. Asthenospheric upwelling due to slab break off after collision could account for this process (Figure 8b) [Oyhantçabal et al., 2007], as in the Western Kunlun orogenic belt in the Tibet Plateau [Ye et al., 2008] and the Alps [von Blanckenburg and Davies, 1995], giving rise to thinning of the lithospheric mantle under the Nico Pérez Terrane and consequent thermal desestabilization [Black and Liégeois, 1993; Liégeois et al., 2013], which is supported by cooling age patterns (Figure 7c) [Oyhantçabal et al., 2011a]. Moreover, significant postcollisional synkinematic magmatism is recorded along the Sarandí del Yí Shear Zone (Figure 5a) and is thus comparable with the magmatism along the Periadriatic Lineament [Steenken et al., 2000; Rosenberg, 2004; Stipp et al., 2004], which also represents a first-order tectonic boundary [Schmid et al., 1989]. Sinistral shearing along the Rivera Shear Zone is recorded in the northern Nico Pérez Terrane at 606 ± 10 Ma as well, indicating coeval antithetic deformation regarding dextral shearing in the Sarandí del Yí Shear Zone (Figure 1) [Oyhantçabal et al., 2012].

The switch from dextral to sinistral shearing along the Sarandí del Yí Shear Zone points to a geodynamic change at approximately 595–590 Ma (Figure 8c). Sinistral shearing is recorded not only in the Sarandí del Yí but also in the Sierra Ballena Shear Zone, which yields $^{40}\text{Ar}/^{39}\text{Ar}$ muscovite ages of 585.8 ± 1.6 Ma [Oyhantçabal *et al.*, 2009b]. The onset of subduction at approximately 595–590 Ma along the northern margin of the Khomas Ocean and/or the southernmost margin of Adamastor Ocean [Prave, 1996; Gray *et al.*, 2008; Rapela *et al.*, 2011] due to the convergence of the Kalahari Craton may provide a satisfactory explanation for this process (Figure 8c), as documented by Lehmann *et al.* [2015]. This plate reorganization could be further supported by the sudden change in the apparent polar wander path of the Congo Craton observed after approximately 590 Ma [Moloto-A-Kenguemba *et al.*, 2008]. An alternative hypothesis consists in considering a change during the postcollisional evolution of the Río de la Plata-Nico Pérez-Congo system. The existence of Neoproterozoic magmatism in the Piedra Alta Terrane [Cingolani *et al.*, 2012] as well as the transition from high-K calc-alkaline to alkaline magmatism in the Dom Feliciano Belt [Oyhantçabal *et al.*, 2007] may indicate the final stages of the postcollisional setting, possibly related to asthenospheric upwelling [Liégeois, 1998; Liégeois *et al.*, 1998]. Nevertheless, a combination of both onset of the convergence of the Kalahari Craton and a postcollisional evolution may be also feasible.

Further deformation after 570 Ma is also recorded in the Sarandí del Yí Shear Zone as well as in the Sierra Ballena and Rivera shear zones [Oyhantçabal *et al.*, 2011b, 2012]. These late events probably resulted from the evolution of the Kaoko and Damara belts during the late Ediacaran and Cambrian [Goscombe *et al.*, 2005; Konopásek *et al.*, 2005; Gray *et al.*, 2006; Oyhantçabal *et al.*, 2011b; Ulrich *et al.*, 2011]. However, most of the shear zones of Uruguay were already exhumed at that time and underwent mostly low-*T* deformation, indicating that they record an older evolution than their African counterparts and deformation migrated toward the east.

The existence of collisional events between approximately 625 and 600 Ma in South America can be further traced to the north along the Transbrasiliano Lineament (Figure 1) [Ganade de Araujo *et al.*, 2014a, 2014b]. This crustal-scale structure has been correlated with the easternmost Pampean Belt in the Sierras Pampeanas, mostly based on geophysical data [e.g., Rapela *et al.*, 2007; Peri *et al.*, 2015]. Nevertheless, the collisional phase of the Pampean Belt was placed at the Lower Cambrian [Rapela *et al.*, 1998, 2007; Siegesmund *et al.*, 2010], which is considerably younger than the collision recorded along the Transbrasiliano Lineament [Ganade de Araujo *et al.*, 2014a, 2014b]. The Sarandí del Yí Shear Zone, in contrast, shows both timing of deformation and kinematics, which are comparable with those recorded along the Transbrasiliano Lineament. Consequently, the amalgamation of the Gondwanic domains in the South American Platform [Brito Neves and Fuck, 2014] was completed at ~600 Ma and resulted from the accretion of African blocks to the eastern margin of the South American older nuclei, i.e., the Amazonas and Río de la Plata cratons, along crustal-scale shear zones.

6. Conclusions

Multithermochronometric and structural data from the mylonites combined with geochronological information from shear zone-related magmatism as well as cooling ages of the adjacent blocks were integrated to constrain the tectonometamorphic evolution of the Sarandí del Yí shear Zone. The onset of the deformation is related to the collision of the Río de la Plata and Nico Pérez Terrane at 630–625 Ma, giving rise to dextral shearing up to 596 Ma along the Sarandí del Yí Shear Zone upper to middle-amphibolite conditions in a postcollisional setting. Subsequent sinistral shearing took place between 594 and 584 Ma under lower amphibolite to upper greenschist facies conditions, which was followed by emplacement of the Sierra de las Ánimas Complex and the Cerro Caperuza granite. This process was temporally associated with voluminous postcollisional magmatism and shear zone activity in the Dom Feliciano Belt. Further deformation under brittle conditions was recorded after approximately 570 Ma and was probably linked to the interaction of the Río de la Plata-Congo and Kalahari Cratons during the evolution of the Pan-African belts.

Additionally, the obtained data reveal the complexity in assessing the age of deformation of long-lived shear zones. Strain partitioning and localization with time, magma emplacement, and fluid circulation were identified as the main processes affecting the isotopic systems. Therefore, multiple geochronometers from the mylonitic belts and their adjacent blocks as well as detailed structural analysis have to be integrated in order to establish solid tectonothermal models of crustal-scale shear zones.

Acknowledgments

Data for this paper are available in the Supporting Information S1. Additional information can be obtained from the corresponding author, Sebastián Oriolo (seba.oriolo@gmail.com and sorio-oriolo@gwdg.de). The authors are indebted to the Iglesias family for the hospitality and logistic support during the field work. Brigitte Dietrich, Franziska Wilsky, Klaus Simon, and Nicole Nolte are greatly acknowledged for the support and the advices during preparation, measurement, and interpretation of the Rb-Sr samples. S. Oriolo thanks DAAD for a long-term PhD scholarship (A/12/75051). The authors also want to thank Claudio Faccenna and Augusto Rapalini for the editorial work, and Renata Schmitt and an anonymous reviewer are acknowledged for critical observations and comments that significantly improved the manuscript.

References

- Almeida, F. F. M., G. Amaral, U. G. Cordani, and K. Kawashita (1973), The Precambrian evolution of the South American cratonic margin, south of Amazonas River, in *The Ocean Basins and Margins*, edited by A. C. M. Nairn, W. H. Kanes, and F. G. Stehli, pp. 411–446, Plenum, New York.
- Basei, M. A. S., H. E. Frimmel, A. P. Nutman, F. Preciozzi, and J. Jacob (2005), A connection between the Neoproterozoic Dom Feliciano (Brazil/Uruguay) and Gariep (Namibia/South Africa) orogenic belts—Evidence from a reconnaissance provenance study, *Precambrian Res.*, *139*, 195–221.
- Basei, M. A. S., H. E. Frimmel, A. P. Nutman, and F. Preciozzi (2008), West Gondwana amalgamation based on detrital zircon ages from Neoproterozoic Ribeira and Dom Feliciano belts of South America and comparison with coeval sequences from SW Africa, in *West Gondwana: Pre-Cenozoic Correlations Across the South Atlantic Region*, edited by R. J. Pankhurst et al., *Geol. Soc. London, Spec. Publ.*, *294*, 239–256.
- Basei, M. A. S., E. Peel, L. Sánchez Bettucci, F. Preciozzi, and A. P. Nutman (2011a), The basement of the Punta del Este Terrane (Uruguay): An African Mesoproterozoic fragment at the eastern border of the South American Río de la Plata craton, *Int. J. Earth Sci.*, *100*, 289–304.
- Basei, M. A. S., M. C. Campos Neto, N. A. Castro, A. P. Nutman, K. Wemmer, M. T. Yamamoto, M. Hueck, L. Osako, O. Siga, and C. R. Pasarelli (2011b), Tectonic evolution of the Brusque Group, Dom Feliciano belt, Santa Catarina, Southern Brazil, *J. South Am. Earth Sci.*, *32*, 324–350.
- Bea, F., P. Montero, F. González-Lodeiro, and C. Talavera (2007), Zircon inheritance reveals exceptionally fast crustal magma generation processes in Central Iberia during the Cambro-Ordovician, *J. Petrol.*, *48*, 2327–2339.
- Black, R., and J. P. Liégeois (1993), Cratons, mobile belts, alkaline rocks and continental lithospheric mantle: The Pan-African testimony, *J. Geol. Soc. London*, *150*, 89–98.
- Blanco, G., H. M. Rajesh, C. Gaucher, G. J. B. Gerns, and F. Chemale Jr. (2009), Provenance of the Arroyo del Soldado Group (Ediacaran to Cambrian, Uruguay): Implications for the paleogeographic evolution of southwestern Gondwana, *Precambrian Res.*, *171*, 57–73.
- Bonamici, C. E., M. C. Kozdon, T. Ushikubo, and J. W. Valley (2014), Intragrain oxygen isotope zoning in titanite by SIMS: Cooling rates and fluid infiltration along the Carthage-Colton Mylonite Zone, Adirondack Mountains, NY, USA, *J. Metamorph. Geol.*, *32*, 71–92.
- Bossi, J., and N. Campal (1992), Magmatismo y tectónica transcurrente durante el Paleozoico inferior del Uruguay, in *Paleozoico Inferior de Ibero-América*, edited by J. Gutiérrez, J. Saavedra, and I. Rábano, pp. 343–356, Univ. de Extremadura, Alicante, Spain.
- Bossi, J., and C. Cingolani (2009), Extension and general evolution of the Río de la Plata Craton, in *Neoproterozoic-Cambrian Tectonics, Global Change and Evolution: A Focus on Southwestern Gondwana*, edited by C. Gaucher et al., pp. 73–85, Elsevier, Amsterdam.
- Bozkurt, E., M. Satir, and Ç. Buğdaycıoğlu (2011), Surprisingly young Rb/Sr ages from the Simav extensional detachment fault zone, northern Menderes Massif, Turkey, *J. Geodyn.*, *52*, 406–431.
- Brito Neves, B. B., and R. A. Fuck (2014), The basement of the South American platform: Half Laurentian (N-NW) + half Gondwanan (E-SE) domains, *Precambrian Res.*, *244*, 75–86.
- Brito Neves, B. B., M. da Costa Campos Neto, and R. A. Fuck (1999), From Rodinia to Western Gondwana: An approach to the Brasiliano-Pan African Cycle and orogenic collage, *Episodes*, *22*(3), 155–166.
- Campal, N., and A. Schipilov (1995), The Illescas bluish quartz rapakivi granite (Uruguay–South America): Some geological features, paper presented at Symposium Rapakivi granites and related rocks, Belen.
- Chamberlain, K. R., and S. A. Bowring (2000), Apatite–feldspar U–Pb thermochronometer: A reliable, mid–range (~450°C), diffusion-controlled system, *Chem. Geol.*, *172*, 173–200.
- Cherniak, D. J. (1993), Lead diffusion in titanite and preliminary results on the effects of radiation damage on Pb transport, *Chem. Geol.*, *110*, 177–194.
- Cherniak, D. J. (2000), Pb diffusion in rutile, *Contrib. Mineral. Petrol.*, *139*, 198–207.
- Cherniak, D. J., and E. B. Watson (2000), Pb diffusion in zircon, *Chem. Geol.*, *172*, 5–24.
- Cingolani, C. A., M. A. S. Basei, J. Bossi, D. Piñero, and N. J. Uriz (2012), U–Pb (LA–ICP–MS) zircon age of the La Paz Granite (Pando Belt, Uruguay): An Upper Neoproterozoic magmatic event in the Río de la Plata Craton, paper presented at 8th South American Symposium on Isotope Geology, Bariloche.
- Cordani, U. G., M. S. D'Agrella-Filho, B. B. Brito Neves, and R. I. F. Trindade (2003), Tearing up Rodinia: The Neoproterozoic palaeogeography of South American cratonic fragments, *Terra Nova*, *15*, 350–359.
- Dahl, P. S. (1997), A crystal-chemical basis for Pb retention and fission-track annealing systematics in U-bearing minerals, with implications for geochronology, *Earth Planet. Sci. Lett.*, *150*, 277–290.
- Dodson, M. H. (1973), Closure temperature in cooling geochronological and petrological systems, *Contrib. Mineral. Petrol.*, *40*, 254–274.
- Dunlap, W. J. (1997), Neocrystallization or cooling? $^{40}\text{Ar}/^{39}\text{Ar}$ ages of white micas from low-grade mylonites, *Chem. Geol.*, *143*, 181–203.
- Eberlei, T., G. Habler, W. Wegner, R. Schuster, W. Körner, M. Thöni, and R. Abart (2015), Rb/Sr isotopic and compositional retentivity of muscovite during deformation, *Lithos*, *227*, 161–178.
- Florisbal, L. M., V. A. Janasi, M. F. Bitencourt, and L. M. Heaman (2012), Space-time relation of post-collisional granitic magmatism in Santa Catarina, southern Brazil: U–Pb LA–MC–ICP–MS zircon geochronology of coeval mafic-felsic magmatism related to the Major Gercino Shear Zone, *Precambrian Res.*, *216–219*, 132–151.
- Foster, D. A., B. D. Goscombe, and D. R. Gray (2009), Rapid exhumation of deep crust in an obliquely convergent orogeny: The Kaoko Belt of the Damara Orogen, *Tectonics*, *28*, TC4002, doi:10.1029/2008TC002317.
- Fragoso Cesar, A. R. S. (1991), Tectônica de placas no ciclo brasiliano: As orogenias dos cinturões Dom Feliciano e Ribeira no Rio Grande do Sul, PhD thesis, Univ. of São Paulo, São Paulo, Brazil.
- Frimmel, H. E., M. A. S. Basei, and C. Gaucher (2011), Neoproterozoic geodynamic evolution of SW-Gondwana: A southern African perspective, *Int. J. Earth Sci.*, *100*, 323–354.
- Frost, B. R., K. R. Chamberlain, and J. C. Schumacher (2000), Sphene (titanite): Phase relations and role as a geochronometer, *Chem. Geol.*, *172*, 131–148.
- Ganade de Araujo, C. E., R. F. Weinberg, and U. G. Cordani (2014a), Extruding the Borborema Province (NE-Brazil): A two-stage Neoproterozoic collision process, *Terra Nova*, *26*, 157–168.
- Ganade de Araujo, C. E., D. Rubatto, J. Hermann, U. G. Cordani, R. Caby, and M. A. S. Basei (2014b), Ediacaran 2500-km-long synchronous deep continental subduction in the West Gondwana Orogen, *Nat. Commun.*, *5*, 5198, doi:10.1038/ncomms6198.
- Gaucher, C. (2000), Sedimentology, palaeontology, and stratigraphy of the Arroyo del Soldado Group (Vendian to Cambrian, Uruguay), *Beringeria*, *26*, 1–120.
- Gaucher, C., S. C. Finney, D. G. Poiré, V. A. Valencia, M. Grove, G. Blanco, K. Pamoukaghlián, and L. Gómez Peral (2008), Detrital zircon age of Neoproterozoic sedimentary successions of Uruguay and Argentina: Insights into the geological evolution of the Río de la Plata Craton, *Precambrian Res.*, *167*, 150–170.

- Gaucher, C., R. Frei, F. Chemale Jr., D. Frei, J. Bossi, G. Martínez, L. Chiglini, and F. Cernuschi (2011a), Mesoproterozoic evolution of the Río de la Plata Craton in Uruguay: At the heart of Rodinia?, *Int. J. Earth Sci.*, *100*, 273–288.
- Gaucher, C., R. Frei, A. N. Sial, and J. Cabrera (2011b), Contrasting Sr isotope composition of Paleo- and Neoproterozoic high-Sr limestone successions from the Nico Pérez terrane, Uruguay, paper presented at Gondwana 14, Búzios.
- Gaucher, C., A. N. Sial, R. Frei, V. P. Ferreira, D. Frei, J. Bossi, and J. Cabrera (2014), Magmatismo anorogénico ediacárico, in *Geología del Uruguay, Tomo 1: Predevónico*, edited by J. Bossi and C. Gaucher, pp. 283–298, Univ. de la Repúb., Montevideo.
- Geisler, T., U. Schaltegger, and F. Tomaschek (2007), Re-equilibration of zircon in aqueous fluids and melts, *Elements*, *3*, 43–50.
- Goscombe, B., and D. R. Gray (2007), The Coastal Terrane of the Kaoko Belt, Namibia: Outboard arc-terrace and tectonic significance, *Precambrian Res.*, *155*, 139–158.
- Goscombe, B., and D. R. Gray (2008), Structure and strain variation at mid-crustal levels in a transpressional orogen: A review of Kaoko Belt structure and the character of West Gondwana amalgamation and dispersal, *Gondwana Res.*, *13*, 45–85.
- Goscombe, B., D. R. Gray, R. Armstrong, D. A. Foster, and J. Vogl (2005), Event geochronology of the Pan-African Kaoko Belt, Namibia, *Precambrian Res.*, *140*, 103.e1–103.e41.
- Gray, D. R., D. A. Foster, B. D. Goscombe, C. W. Passchier, and R. A. J. Trouw (2006), $^{40}\text{Ar}/^{39}\text{Ar}$ thermochronology of the Pan-African Damara Orogen, Namibia, with implications for tectonothermal and geodynamic evolution, *Precambrian Res.*, *150*, 49–72.
- Gray, D. R., D. A. Foster, J. G. Meert, B. D. Goscombe, R. Armstrong, R. A. J. Trouw, and C. W. Passchier (2008), A Damara orogeny perspective on the assembly of southwestern Gondwana, in *West Gondwana: Pre-Cenozoic Correlations Across the South Atlantic Region*, edited by R. J. Pankhurst et al., *Geol. Soc. London, Spec. Publ.*, *294*, 257–278.
- Gross, A. O. M. S., C. C. Porcher, L. A. D. Fernandes, and E. Koester (2006), Neoproterozoic low-pressure/high-temperature collisional metamorphic evolution in the Varzea do Capivarita Metamorphic Suite, SE Brazil: Thermobarometric and Sm/Nd evidence, *Precambrian Res.*, *147*, 41–64.
- Harrison, T. M. (1981), Diffusion of ^{40}Ar in hornblende, *Contrib. Mineral. Petrol.*, *78*, 324–331.
- Harrison, T. M., I. Duncan, and I. McDougall (1985), Diffusion of ^{40}Ar in biotite: Temperature, pressure and compositional effects, *Geochim. Cosmochim. Acta*, *49*, 2461–2468.
- Harrison, T. M., J. Célérier, A. B. Aikman, J. Hermann, and M. T. Heizler (2009), Diffusion of ^{40}Ar in muscovite, *Geochim. Cosmochim. Acta*, *73*, 1039–1051.
- Hartmann, L. A., D. Piñeyro, J. Bossi, J. A. D. Leite, and N. J. McNaughton (2000), Zircon U-Pb SHRIMP dating of Palaeoproterozoic Isla Mala granitic magmatism in the Río de la Plata Craton, Uruguay, *J. South Am. Earth Sci.*, *13*, 105–113.
- Hartmann, L. A., N. Campal, J. O. S. Santos, N. J. McNaughton, J. Bossi, A. Schipilov, and J.-M. Lafon (2001), Archean crust in the Río de la Plata Craton, Uruguay, *J. South Am. Earth Sci.*, *14*, 557–570.
- Hartmann, L. A., J. O. S. Santos, J. Bossi, N. Campal, A. Schipilov, and N. J. McNaughton (2002), Zircon and titanite U-Pb SHRIMP geochronology of Neoproterozoic felsic magmatism on the eastern border of the Río de la Plata Craton, Uruguay, *J. South Am. Earth Sci.*, *15*, 229–236.
- Heaman, L., and R. R. Parrish (1991), U-Pb geochronology on accessory minerals, in *Applications of Radiogenic Isotope Systems to Problems in Geology*, edited by L. Heaman and J. N. Ludden, pp. 59–102, Mineral. Assoc. of Canada, Toronto.
- Hoskin, P. W. O., and U. Schaltegger (2003), The composition of zircon and igneous and metamorphic petrogenesis, in *Zircon, Reviews in Mineralogy & Geochemistry*, vol. 53, edited by J. M. Hancher and P. W. O. Hoskin, pp. 27–62, Mineral. Soc. of Am., Washington, D. C.
- Jäger, E. (1977), Introduction to geochronology, in *Lectures of Isotope Geology*, edited by E. Jäger and J. Hunziker, pp. 1–12, Springer, Heidelberg, Germany.
- Jäger, E., E. Niggli, and E. Wenk (1967), *Rb-Sr Altersbestimmungen an Glimmern der Zentralalpen, Beiträge zur Geologischen Karte der Schweiz*, vol. 134, Kümmerly & Frey, Bern.
- Jenkin, G. R. T. (1997), Do cooling paths derived from mica Rb-Sr data reflect true cooling paths? *Geology*, *25*(10), 907–910.
- Konopásek, J., S. Kröner, S. L. Kitt, C. W. Passchier, and A. Kröner (2005), Oblique collision and evolution of large-scale transcurrent shear zones in the Kaoko belt, NW Namibia, *Precambrian Res.*, *139*, 139–157.
- Konopásek, J., J. Košler, L. Tajčmanová, S. Ulrich, and S. L. Kitt (2008), Neoproterozoic igneous complex emplaced along major tectonic boundary in the Kaoko Belt (NW Namibia): Ion probe and LA-ICP-MS dating of magmatic and metamorphic zircons, *J. Geol. Soc. London*, *165*, 153–165.
- Konopásek, J., J. Košler, J. Sláma, and V. Janoušek (2014), Timing and sources of pre-collisional Neoproterozoic sedimentation along the SW margin of the Congo Craton (Kaoko Belt, NW Namibia), *Gondwana Res.*, *26*, 386–401.
- Kooijman, E., K. Mezger, and J. Berndt (2010), Constraints on the U-Pb systematics of metamorphic rutile from in situ LA-ICP-MS analysis, *Earth Planet. Sci. Lett.*, *293*, 321–330.
- Kröner, A., and R. J. Stern (2004), Pan-African orogeny, in *Encyclopedia of Geology*, edited by R. C. Selley, L. R. M. Cocks, and I. R. Plimer, pp. 1–12, Elsevier, Amsterdam.
- Kröner, S., J. Konopásek, A. Kröner, C. W. Passchier, U. Poller, M. W. D. Wingate, and K. H. Hofmann (2004), U-Pb and Pb-Pb zircon ages for metamorphic rocks in the Kaoko Belt of Northwestern Namibia: A Palaeo- to Mesoproterozoic basement reworked during the Pan-African orogeny, *S. Afr. J. Geol.*, *107*, 455–476.
- Kruhl, J. H. (1996), Prism- and basal-plane parallel subgrain boundaries in quartz: A microstructural geothermobarometer, *J. Metamorph. Geol.*, *14*, 581–589.
- Lara, P., P. Oyhançabal, K. Dadd, and C. Rossini (2013), Late Neoproterozoic high Barium-Strontium granitic magmatism of the Precambrian Uruguayan Shield, paper presented at 7th Congreso Uruguayo de Geología and 1st Simposio de Minería y Desarrollo del Cono Sur, Sociedad Uruguay de Geología, Montevideo.
- Lehmann, J., K. Saalman, K. V. Naydenov, L. Milani, G. A. Belyanin, H. Zwingmann, G. Charlesworth, and J. A. Kinnaird (2015), Structural and geochronological constraints of the Pan-African tectonic evolution of the northern Damara Belt, Namibia, *Tectonics*, *35*, 103–135, doi:10.1002/2015TC003899.
- Lenz, C., L. A. D. Fernandes, N. J. McNaughton, C. C. Porcher, and H. Masquelin (2011), U-Pb SHRIMP ages for the Cerro Bori Orthogneisses, Dom Feliciano Belt in Uruguay: Evidences of a ~800 Ma magmatic and a ~650 Ma metamorphic event, *Precambrian Res.*, *185*, 149–163.
- Liégeois, J. P. (1998), Preface—Some words on the postcollisional magmatism, *Lithos*, *45*, XV–XVII.
- Liégeois, J. P., J. Navez, J. Hertogen, and R. Black (1998), Contrasting origin of post-collisional high-K calc-alkaline and shoshonitic versus alkaline and peralkaline granitoids. The use of sliding normalization, *Lithos*, *45*, 1–28.
- Liegeois, J. P., M. G. Abdesalam, N. Ennih, and A. Ouabadi (2013), Metacraton: Nature, genesis and behavior, *Gondwana Res.*, *23*, 220–237.
- Maki, K., T.-F. Yui, K. Miyazaki, M. Fukuyama, K.-L. Wang, U. Martens, M. Grove, and J. G. Liou (2014), Petrogenesis of metatexite and diatexite migmatites determined using zircon U-Pb age, trace element and Hf isotope data, Higo metamorphic terrane, central Kyushu, Japan, *J. Metamorph. Geol.*, *32*, 301–323.

- Mallmann, G., F. Chemale Jr., J. N. Ávila, K. Kawashita, and R. A. Armstrong (2007), Isotope geochemistry and geochronology of the Nico Pérez Terrane, Rio de la Plata Craton, Uruguay, *Gondwana Res.*, **12**, 489–508.
- Mezger, K., E. J. Essene, and A. N. Halliday (1992), Closure temperatures of the Sm–Nd system in metamorphic garnets, *Earth Planet. Sci. Lett.*, **193**, 397–409.
- Moloto-A-Kenguemba, G. R., R. I. F. Trindade, P. Monié, A. Nédélec, and R. Siquiera (2008), A late Neoproterozoic paleomagnetic pole for the Congo craton: Tectonic setting, paleomagnetism and geochronology of the Nola dike swarm (Central African Republic), *Precambrian Res.*, **164**, 214–226.
- Montaña, J., and P. Sprechmann (1993), Calizas estromatolíticas y oolíticas y definición de la Formación Arroyo de la Pedrera (?Vendiano, Uruguay), *Rev. Bras. Geocienc.*, **23**, 306–312.
- Mulch, A., and M. A. Cosca (2004), Recrystallization or cooling ages: In situ UV-laser $^{40}\text{Ar}/^{39}\text{Ar}$ geochronology of muscovite in mylonitic rocks, *J. Geol. Soc. London*, **161**, 573–582.
- Mulch, A., C. Teysier, M. A. Cosca, and T. W. Vennemann (2006), Thermomechanical analysis of strain localization in a ductile detachment zone, *J. Geophys. Res.*, **111**, B12405, doi:10.1029/2005JB004032.
- Oriolo, S., P. Oyhançabal, F. Heidelbach, K. Wemmer, and S. Siegesmund (2015), Structural evolution of the Sarandí del Yí Shear Zone: Kinematics, deformation conditions and tectonic significance, *Int. J. Earth Sci.*, **104**, 1759–1777, doi:10.1007/s00531-015-1166-2.
- Oyhançabal, P. (2005), The Sierra Ballena shear zone: Kinematics, timing and its significance for the geotectonic evolution of southeast Uruguay, Ph. D. thesis, Dept. of Struc. Geol. and Geodyn., Georg-August-Univ. Göttingen, Göttingen, Germany.
- Oyhançabal, P., R. Muzio, and S. de Souza (1993), Geología y aspectos estructurales del borde orogénico en el extremo sur del cinturón Don Feliciano, *Rev. Bras. Geocienc.*, **23**, 296–300.
- Oyhançabal, P., A. Heimann, and S. Miranda (2001), Measurement and interpretation of strain in the syntectonic Solís de Mataojo Granitic Complex, Uruguay, *J. Struct. Geol.*, **23**, 807–817.
- Oyhançabal, P., L. Sánchez Bettucci, E. Pecoits, N. Aubet, E. Peel, F. Preciozzi, and M. A. S. Basei (2005), Nueva propuesta estratigráfica para las supracorticales del Cinturón Dom Feliciano (Proterozoico Uruguay), paper presented at 12th Congreso Latinoamericano de Geología, Quito.
- Oyhançabal, P., S. Siegesmund, K. Wemmer, R. Frei, and P. Layer (2007), Post-collisional transition from calc-alkaline to alkaline magmatism during transcurrent deformation in the southernmost Dom Feliciano Belt (Braziliano–Pan–African, Uruguay), *Lithos*, **98**, 141–159.
- Oyhançabal, P., S. Siegesmund, K. Wemmer, S. Presnyakov, and P. Layer (2009a), Geochronological constraints on the evolution of the southern Dom Feliciano Belt (Uruguay), *J. Geol. Soc. London*, **166**, 1075–1084.
- Oyhançabal, P., S. Siegesmund, K. Wemmer, and P. Layer (2009b), The Sierra Ballena Shear Zone in the southernmost Dom Feliciano Belt (Uruguay): Evolution, kinematics, and deformation conditions, *Int. J. Earth Sci.*, doi:10.1007/s00531-009-0453-1.
- Oyhançabal, P., S. Siegesmund, and K. Wemmer (2011a), The Río de la Plata Craton: A review of units, boundaries, ages and isotopic signature, *Int. J. Earth Sci.*, **100**, 201–220.
- Oyhançabal, P., S. Siegesmund, K. Wemmer, and C. W. Passchier (2011b), The transpressional connection between Dom Feliciano and Kaoko Belts at 580–550 Ma, *Int. J. Earth Sci.*, **100**, 379–390.
- Oyhançabal, P., M. Wegner-Eimer, K. Wemmer, B. Schulz, R. Frei, and S. Siegesmund (2012), Paleo- and Neoproterozoic magmatic and tectonometamorphic evolution of the Isla Cristalina de Rivera (Nico Pérez Terrane, Uruguay), *Int. J. Earth Sci.*, **101**, 1745–1762.
- Passchier, C. W., and R. A. J. Trouw (2005), *Microtectonics*, 2nd ed., Springer, Berlin.
- Peel, E., and F. Preciozzi (2006), Geochronological synthesis of the Piedra Alta Terrane, Uruguay, paper presented at 5th South American Symposium on Isotope Geology, Punta del Este.
- Peri, V. G., H. Barcelona, M. C. Pomposiello, and A. Favetto (2015), Magnetotelluric characterization through the Ambargasta-Sumampa Range: The connection between the northern and southern trace of the Río de la Plata Craton–Pampean Terrane tectonic boundary, *J. South Am. Earth Sci.*, **59**, 1–12.
- Philipp, R. P., H.-J. Massonne, and R. Sacks de Campos (2013), Peraluminous leucogranites of the Cordilheira Suite: A record of Neoproterozoic collision and the generation of the Pelotas Batholith, Dom Feliciano Belt, Southern Brazil, *J. South Am. Earth Sci.*, **43**, 8–24.
- Prave, A. R. (1996), Tale of three cratons: Tectonostratigraphic anatomy of the Damara orogen in northwestern Namibia and the assembly of Gondwana, *Geology*, **24**(12), 1115–1118.
- Preciozzi, F., J. Spoturno, and W. Heinzen (1979), Carta geo-estructural del Uruguay, escala 1:2.000.000, Inst. Geol. Ing. Terra Arocena, Montevideo.
- Pryer, L. L. (1993), Microstructures in feldspars from a major crustal thrust zone: The Grenville Front, Ontario, Canada, *J. Struct. Geol.*, **15**, 21–36.
- Purdy, J. W., and E. Jäger (1976), K–Ar ages on rock-forming minerals from the Central Alps, *Mem. Ist. Geol. Mineral. Univ. Padova*, **30**, 1–31.
- Rapalini, A. E., and L. Sánchez Bettucci (2008), Widespread remagnetization of late Proterozoic sedimentary units of Uruguay and the apparent polar wander path for the Río de la Plata craton, *Geophys. J. Int.*, **174**, 55–74.
- Rapalini, A. E., E. Tohver, L. Sánchez Bettucci, A. C. Lossada, H. Barcelona, and C. Pérez (2015), The late Neoproterozoic Sierra de las Ánimas Magmatic Complex and Playa Hermosa Formation, southern Uruguay, revisited: Paleogeographic implications of new paleomagnetic and precise geochronologic data, *Precambrian Res.*, **259**, 143–155.
- Rapela, C. W., R. J. Pankhurst, C. Casquet, E. G. Baldo, J. Saavedra, C. Galindo, and C. M. Fanning (1998), The Pampean Orogeny of the southern proto-Andes: Cambrian continental collision in the Sierras de Córdoba, in *The Proto-Andean Margin of Gondwana*, edited by R. J. Pankhurst and C. W. Rapela, *Geol. Soc. London, Spec. Publ.*, **142**, 181–217.
- Rapela, C. W., R. J. Pankhurst, C. Casquet, C. M. Fanning, E. G. Baldo, J. M. González-Casado, C. Galindo, and J. Dahlquist (2007), The Río de la Plata craton and the assembly of SW Gondwana, *Earth Sci. Rev.*, **83**, 49–82.
- Rapela, C. W., C. M. Fanning, C. Casquet, R. J. Pankhurst, L. Spalletti, D. Poiré, and E. G. Baldo (2011), The Río de la Plata craton and the adjoining Pan-African/braziliano terranes: Their origins and incorporation into south-west Gondwana, *Gondwana Res.*, **20**, 673–690.
- Rolland, Y., M. Rossi, S. F. Cox, M. Corsini, N. Mancktelow, G. Pennacchioni, M. Fornari, and A. M. Boullier (2008), $^{40}\text{Ar}/^{39}\text{Ar}$ dating of synkinematic white data: Insights from fluid-rock reaction in low-grade shear zones (Mont Blanc Massif) and constraints on timing of deformation in the NW external Alps, in *The Internal Structure of Fault Zones: Implications for Mechanical and Fluid-Flow Properties*, edited by C. A. J. Wibberley et al., *Geol. Soc. London, Spec. Publ.*, **299**, 293–315.
- Rosenberg, C. L. (2004), Shear zones and magma ascent: A model based on a review of the Tertiary magmatism in the Alps, *Tectonics*, **23**, TC3002, doi:10.1029/2003TC001526.
- Sánchez Bettucci, L., F. Preciozzi, M. A. S. Basei, P. Oyhançabal, E. Peel, and J. Loureiro (2003), Campanero Unit: A probable Paleoproterozoic basement and its correlation to other units of southeastern Uruguay, paper presented at 4th South American Symposium on Isotope Geology, Salvador.
- Sánchez Bettucci, L., P. Oyhançabal, J. Loureiro, V. A. Ramos, F. Preciozzi, and M. A. S. Basei (2004), Mineralizations of the Lavalaja group (Uruguay), a probable neoproterozoic volcano-sedimentary sequence, *Gondwana Res.*, **6**, 89–105.

- Sánchez Bettucci, L., E. Masquelin, E. Peel, P. Oyhantçabal, R. Muzio, J. J. Ledesma, and F. Preciozzi (2010), Comment on "Provenance of the Arroyo del Soldado Group (Ediacaran to Cambrian, Uruguay): Implications for the paleogeographic evolution of southwestern Gondwana" by Blanco et al. [*Precambrian Res.* 171 (2009) 57–63], *Precambrian Res.*, 180, 328–333.
- Santos, J. O. S., L. A. Hartmann, J. Bossi, N. Campal, A. Schipilov, D. Piñeyro, and N. J. McNaughton (2003), Duration of the Trans-Amazonian cycle and its correlation within South America based on U-Pb SHRIMP geochronology of the La Plata Craton, Uruguay, *Int. Geol. Rev.*, 45, 27–48.
- Schmid, S. M., H. R. Aebli, F. Heller, and A. Zingg (1989), The role of the Periadriatic Line in the tectonic evolution of the Alps, in *Alpine Tectonics*, edited by M. P. Coward, D. Dietrich, and R. G. Park, *Geol. Soc. London. Spec. Publ.*, 45, 153–171.
- Seth, B., A. Kröner, K. Mezger, A. A. Nemchin, R. T. Pidgeon, and M. Okrusch (1998), Archean to Neoproterozoic magmatic events in the Kaoko Belt of NW Namibia and their geodynamic significance, *Precambrian Res.*, 92, 341–363.
- Siegesmund, S., A. Steenken, R. D. Martino, K. Wemmer, M. López de Luchi, R. Frei, S. Presnyakov, and A. Guerreschi (2010), Time constraints on the tectonic evolution of the Eastern Sierras Pampeanas (Central Argentina), *Int. J. Earth Sci.*, 99, 1199–1226.
- Spoturno, J. J., P. Oyhantçabal, C. Goso, N. Aubet, and S. Cazaux (2011), Mapa geológico y de recursos minerales del Departamento de Canelones a escala 1:100.000, Proyecto CONICYT 6019, Montevideo.
- Spoturno, J. J., P. Oyhantçabal, and J. Loureiro (2012), Mapa geológico del Departamento de Maldonado escala 1:100.000, Facultad de Ciencias (UdelaR)–Dirección Nacional de Minería y Geología (MIEM), Montevideo.
- Steenken, A., S. Siegesmund, and T. Heinrichs (2000), The emplacement of the Rieserferner Pluton (Eastern Alps, Tyrol): Constraints from field observations, magnetic fabrics and microstructures, *J. Struct. Geol.*, 22, 1855–1873.
- Stipp, M., H. Stünitz, R. Heilbronner, and S. M. Schmid (2002), The eastern Tonale fault: A "natural laboratory" for crystal plastic deformation of quartz over a temperature range from 250 to 700°C, *J. Struct. Geol.*, 24, 1861–1884.
- Stipp, M., B. Fügenschuh, L. P. Gromet, H. Stünitz, and S. M. Schmid (2004), Contemporaneous plutoning and strike-slip faulting: A case study from the Tonale fault zone north of the Adamello Pluton (Italian Alps), *Tectonics*, 23, TC3004, doi:10.1029/2003TC001515.
- Teixeira, W., P. R. Renne, J. Bossi, N. Campal, and M. S. D'Agrella Filho (1999), ⁴⁰Ar–³⁹Ar and Rb–Sr geochronology of the Uruguayan dike swarm, Rio de la Plata Craton and implications for Proterozoic intraplate activity in western Gondwana, *Precambrian Res.*, 93, 153–180.
- Teixeira, W., M. S. D'Agrella Filho, M. Hamilton, R. E. Ernst, V. A. V. Girardi, M. Mazzuchelli, and J. S. Bethencourt (2013), U–Pb (ID-TIMS) baddeleyite ages and paleomagnetism of 1.79 and 1.59 Ga tholeiitic dyke swarms, and position of the Rio de la Plata Craton within the Columbia supercontinent, *Lithos*, 174, 157–174.
- Tibaldi, A. M., J. E. Otamendi, E. A. Cristofolini, I. Baliani, B. A. Walker Jr., and G. W. Bergantz (2013), Reconstruction of the Early Ordovician Famatinian arc through thermobarometry in lower and middle crustal exposures, Sierra de Valle Fértil, Argentina, *Tectonophysics*, 589, 151–166.
- Ulrich, S., J. Konopásek, P. Jeřábek, and L. Tajčmanová (2011), Transposition of structures in the Neoproterozoic Kaoko Belt (NW Namibia) and their absolute timing, *Int. J. Earth Sci.*, 100, 415–429.
- Umpierre, M., and M. Halpern (1971), Edades Sr–Rb del Sur de la República Oriental del Uruguay, *Rev. Asoc. Geol. Argent.*, 26, 133–151.
- van der Pluijm, B. A., K. Mezger, M. A. Cosca, and E. J. Essene (1994), Determining the significance of high-grade shear zones by using temperature-time paths, with examples from the Grenville orogen, *Geology*, 22, 743–746.
- Villa, I. M. (1998), Isotopic closure, *Terra Nova*, 10, 42–47.
- Voll, G. (1976), Recrystallization of quartz, biotite and feldspars from Erstfeld to the Leventina nappe, Swiss Alps, and its geological significance, *Schweiz. Mineral. Petrogr. Mitt.*, 56, 641–647.
- von Blanckenburg, F., and J. H. Davies (1995), Slab breakoff: A model for syncollisional magmatism and tectonics in the Alps, *Tectonics*, 14, 120–131, doi:10.1029/94TC02051.
- Vry, J. K., and J. A. Baker (2006), LA-MC-ICPMS Pb–Pb dating of rutile from slowly cooled granulites: Confirmation of the high closure temperature for Pb diffusion in rutile, *Geochim. Cosmochim. Acta*, 70, 1807–1820.
- Ye, H.-M., X.-H. Li, Z.-X. Li, and C.-L. Zhang (2008), Age and origin of high Ba–Sr appinite-granites at the northwestern margin of the Tibet Plateau: Implications for early Paleozoic tectonic evolution of the Western Kunlun orogenic belt, *Gondwana Res.*, 13, 126–138.